AD-A055 036 NAVAL INTELLIGENCE SUPPORT CENTER WASHINGTON D C TRA--ETC F/G 14/5
TIME AND LATITUDE DETERMINATIONS WITH THE PHOTOGRAPHIC ZENITH T--ETC(U)
MAR 78 M MEINIG, H JACHMANN

UNCLASSIFIED NISC-TRANS-4008 NL

| OF |

AD
A055036

END
DATE
FILMED
7-78
DDC

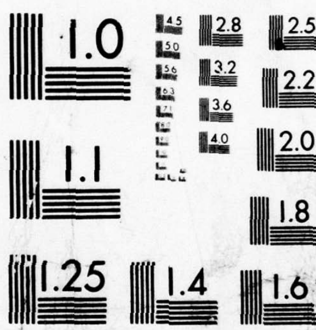

MICROCOPY RESOLUTION TEST CHART
NATIONAL BUREAU OF STANDARDS-1963-A

AD A055036

DEPARTMENT OF THE NAVY
NAVAL INTELLIGENCE SUPPORT CENTER
TRANSLATION DIVISION
4301 SUITLAND ROAD
WASHINGTON, D.C. 20390

CLASSIFICATION: UNCLASSIFIED

TITLE: (6) Time and Latitude Determinations with the Photographic Zenith Telescope of the Central Geophysics Institute

(Zeit-und Breitenbestimmungen mit dem photografischen Zenitteleskop des Zentralinstituts für Physik der Erde)

AUTHOR(S): Meinig, Manfred and Jachmann, Horst

PAGES: ~~64~~ (21) Trans. of

SOURCE: Academy of Sciences of the German Democratic Republic
Publications of the Central Geophysics Institute No. 49
[redacted]
(East Germany) n49 p3-59 N.D.

(10) Manfred /Meinig
Horst /Jachmann

ORIGINAL LANGUAGE: German

TRANSLATOR: C

NISC TRANSLATION NO. 4008 ✓

APPROVED P.T.K.

DATE (11) 14 March 1978

(14) NISC-TRANS-4008

(12) 68p.

407 682

LB

ACADEMY OF SCIENCES OF THE GERMAN DEMOCRATIC REPUBLIC
PUBLICATIONS OF THE CENTRAL GEOPHYSICS INSTITUTE NO. 49

TIME AND LATITUDE DETERMINATIONS WITH THE PHOTOGRAPHIC ZENITH TELESCOPE OF THE CENTRAL GEOPHYSICS INSTITUTE

by Manfred Meinig and Horst Jochmann

Printed as Manuscript, Potsdam 1976

TABLE OF CONTENTS | Page

SUMMARY

Since 1972, observations with the PZT have been carried out regularly in Potsdam. The principles of construction and the operating mode of the instrument are described. From the fundamental relations between image point coordinates, star positions and station coordinates, the imaging equations are developed and the basic formulas for the evaluation are derived therefrom. The influence of azimuth and reversal errors on the time and latitude determination is examined from the point of view of error theory. For the reduction of the observations, star locations are used since 1974, which were improved on the basis of the results of 1972 and 1973. In an accuracy analysis, the influence of various sources of error are examined and the efficiency of the instrument is estimated. The random errors obtained in time and latitude determinations are compared with the values which can be expected theoretically. The results for 1972 to 1974 are summarized in the appendix.

1. INTRODUCTION

The photographic zenith telescope (PZT) is used as an efficient instrument for geodetic-astronomical time and latitude determinations at fixed stations for the determination of data for the investigation of the rotating behavior of the earth. In comparison with other types of instruments, which are used for the same purpose, the PZT has some advantages.

Because the observation process is performed automatically and is controlled by a program circuit, human errors have no effect in the observation and the observer is largely relieved. His activity consists of the preparation of the instrument, of the time recording apparatus and of the program controller, the insertion of the cassette, the starting of the program at the predetermined point in time, the control and monitoring of the program operation and the removal of the cassette at the

completion of the observation.

Because of the observation in the immediate vicinity of the zenith, refraction errors play a subordinate role. Their influence is further reduced by the method of evaluation and by the configuration of the star program. Influences of instrument errors are also largely eliminated by the principle of construction of the PZT. The specified tolerances for installation and adjustment can be maintained without difficulty. Last but not least, the PZT is superior to the other types of instruments because of its greater dimensions in comparison with the passage instrument and Astrolab.

One disadvantage of the PZT results from the fact that the observation is carried out only in the immediate vicinity of the zenith and stars can therefore only be observed in a small declination zone. Therefore, fundamental stars are hardly available and the program must be composed of stars of which the locations and inherent motions are initially not known with adequate accuracy and must still be improved with the aid of PZT observations and special observations. Another disadvantage consists of the use of the photographic plate as intermediate storage, which makes the evaluation process very time-consuming.

The PZT, which was built in the institute workshop of the observatory Babelsberg (Figure 1), was tested by the Geodetic-Astronomical Observatory of the Central Geophysical Institute following acceptance. Some instrument improvements have been carried out on the basis of experiences accumulated during the experimental observations. The instrument is installed in the west meridian house on the grounds of the observatory in Babelsberg. Sice 1972, it has been used regularly for time and latitude determinations.

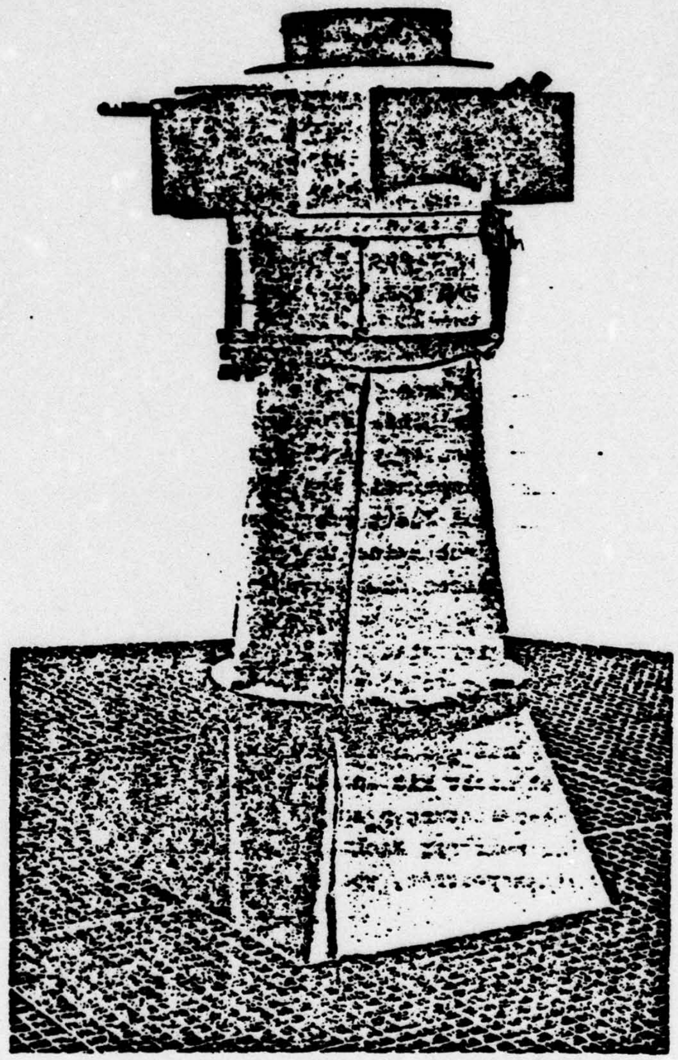

Figure 1. The Photographic Zenith Telescope

2. PRINCIPLE OF CONSTRUCTION AND OPERATING MODE OF THE INSTRUMENT

In comparison with other instruments for the geodetic-astronomical locus and time determination, the PZT is excels by the optimum elimination of the influence of instrument errors.

All more accurate observation methods of geodetic astronomy are based on the stabilization of the azimuth circles or almucantars defined by the observation instrument during the transit of the star. In the case of the PZT, which has a vertical optical axis, the stabilization is carried out by a mercury horizon located in the half focal distance. The image plane is located in the image-side principal plane of the objective, which assures that depth errors between mercury horizon and objective can have no technical effect. They would only have the effect of a deterioration of the image quality on the photographic plate.

The fundamental optical configuration of the PZT is illustrated in Figure 2. After the rays have passed the objective 1, they are reflected on the mercury horizon 2 and produce an image on the photographic plate 3, which is located in the image-side principal plane of the objective and can be moved in the west-east direction. The evaluation principle of the PZT requires that four images are produced for each star transit, whereby, between the individual exposures, the head of the instrument must be turned by 180°. Follow-up of the photographic plate and rotation of the head of the instrument between the individual observations are carried out automatically during the observation cycle.

As shown in the following chapter, the zenith distance and the meridian transit time can be determined from the coordinate differences of the four images, which are produced during a star transit, if the mean time of the four exposures is given.

The time pattern of the observation of the transit of a star is illustrated in Figure 3. The total observation cycle takes 120 seconds, each exposure 20 seconds, and the instrument head is turned within 10 seconds. All necessary motions and control commands are carried out automatically by the drive mechanism (Figure 4).

When the starting impulse is initiated, the starting magnet 5 pulls in the gear coupling 15 and connects the cycle drive 4 with the second shaft 2. The speed reduction from the second shaft to the cycle drive is 30:1. After 5 seconds, the contact is closed by the cycle drive. In this manner, the bevel gear return drive 3 for the transport of the plate stage is coupled through the coupling magnet 9. At the same time, the exposure shutter is opened. The coupling of the bevel gear return drive takes place through follower pins 14, whereby the coupling takes place for left-hand or right-hand operation, depending on the position of the instrument head. With respect to the second shaft, the bevel gear return drive is operating at a reduction of 2:1. The drive spindle 7, which rotates with the bevel gear, moves a nut 8, through which the plate stage 13, which is pressed against the moving mechanism by means of spring force, is moved. The drive spindle has a pitch, which is adapted to the geographical latitude of the location of the installation.

In addition to the plate stage, the drive spindle rotates a shaft, at a ratio of 20:1, with cams 6, which are used to energize the stop contact and the relay circuit for the reversal of the instrument head. After reversal, which takes 7 seconds, a new exposure cycle is initiated after 3 seconds. The observation is stopped through a time relay in the control device. A piacrylic disc 11 is connected with the drive shaft, serving as time contact generator. This piacrylic disc has a light gap, permitting the passage of light, which comes from a lamp with optical imaging device 12, at an appropriate position of the disc and thus makes possible the imaging of the lamp

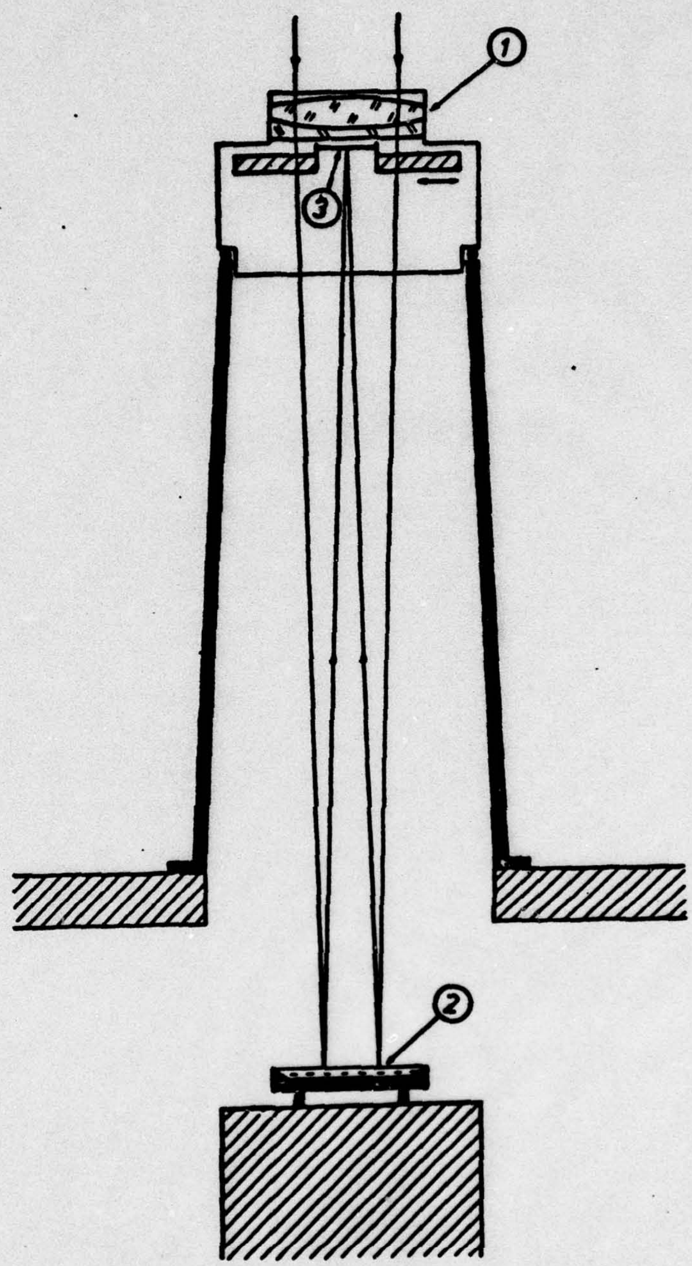

Figure 2. Optical Construction of the PZT

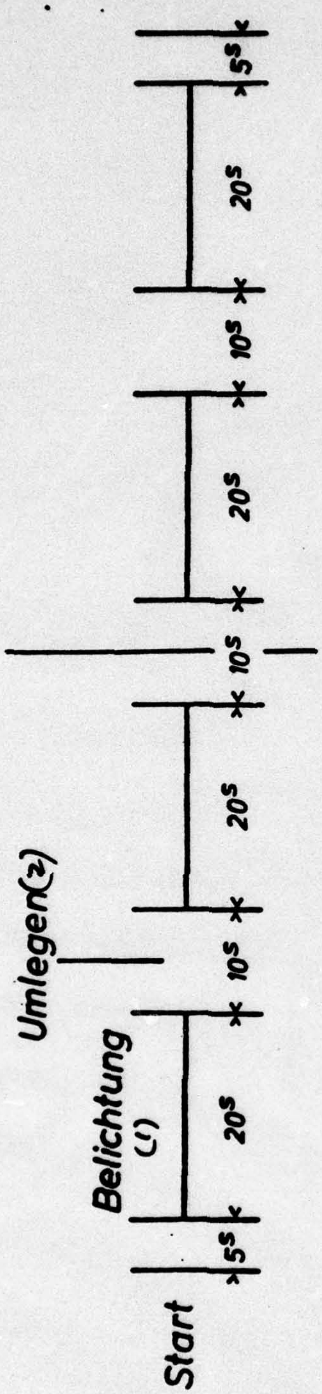

Figure 3. Time Pattern of the Instrument Functions During A Star Transit

Key:

1. Exposure
2. Motion (reversal or rotation)

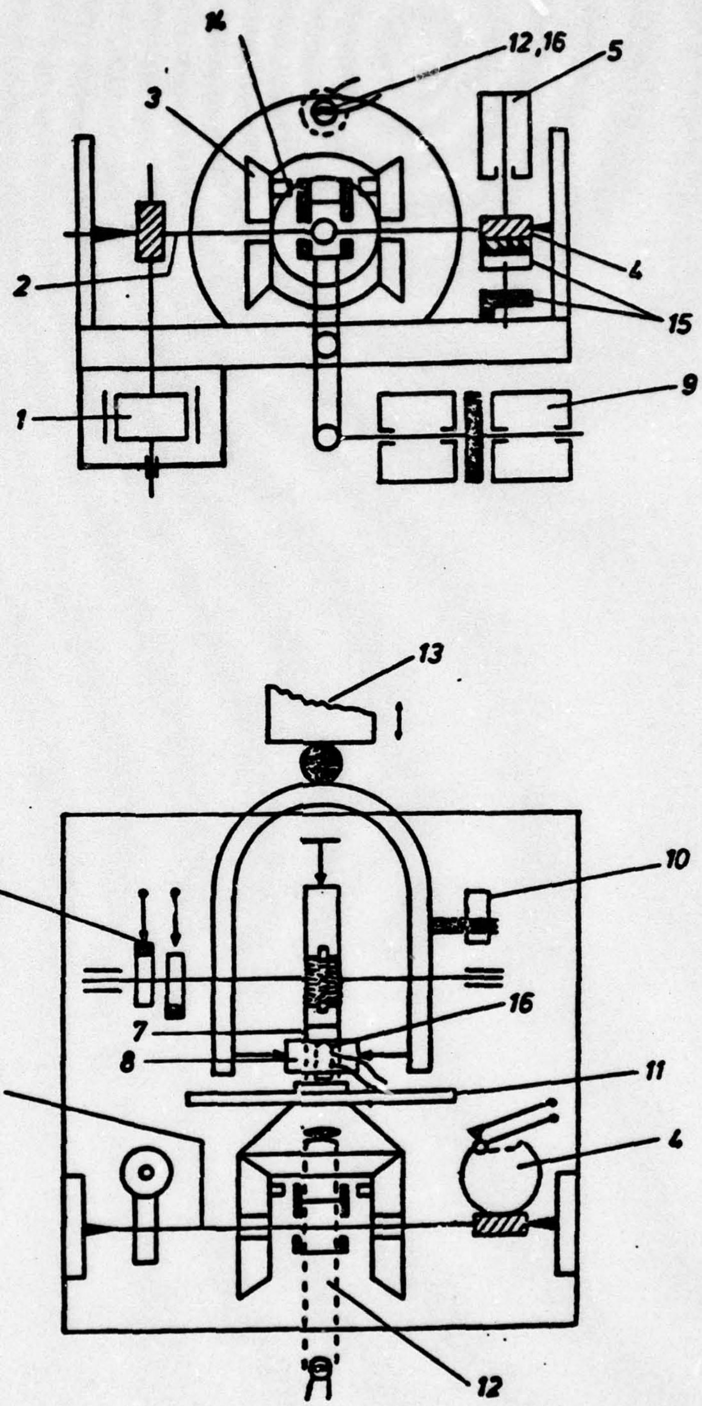

Figure 4. The Drive Mechanism (schematic) of the PZT Plate Stage (according to Engelbrecht (1))

coil on a photodiode. This produces a starting impulse, which initiates an electronic time interval metering device. It obtains the stopping impulse through the second contacts of the time service of the geodetic-astronomical observatory. During the rotation of the drive spindle, the fractions of seconds of a point in time are recorded per exposure in this manner. The mean of the four recorded times corresponds to the fractions of seconds of the mean time of the observation cycle. The second shaft 2 is driven by a 1000 Hz synchronous motor 1, which is controlled by the normal frequency of a quarz clock.

The functional diagram of the PZT is illustrated in Figure 5. The components illustrated below the dotted line are located on the instrument, while those above the line are accomodated in a separate control room.

The observation cycle can be initiated for each star by manual starting, or it can be initiated for the entire program of a night by means of the program generator. The above-described configuration of the drive mechanism and its association with the time contact generation assure a realtionship of the star images with the time contact, which is largely uninfluenced by adjustment errors.

If, during an exposure, a time interval Δt elapses from the beginning of the motion to the time contact generation, the time interval in the instrument head in the position which is rotated by 180°, amounts to $2s - \Delta t$. The mean of the time recordings of all four exposures would thus result in the time mean of the exposures, which are displaced by 1 second. However, this necessary correction has no significance for the evaluation of the PZT observation, because fractions of seconds are taken into consideration anyway.

In a manner similar to the time interval from the beginning of the motion to the time contact generation, the different

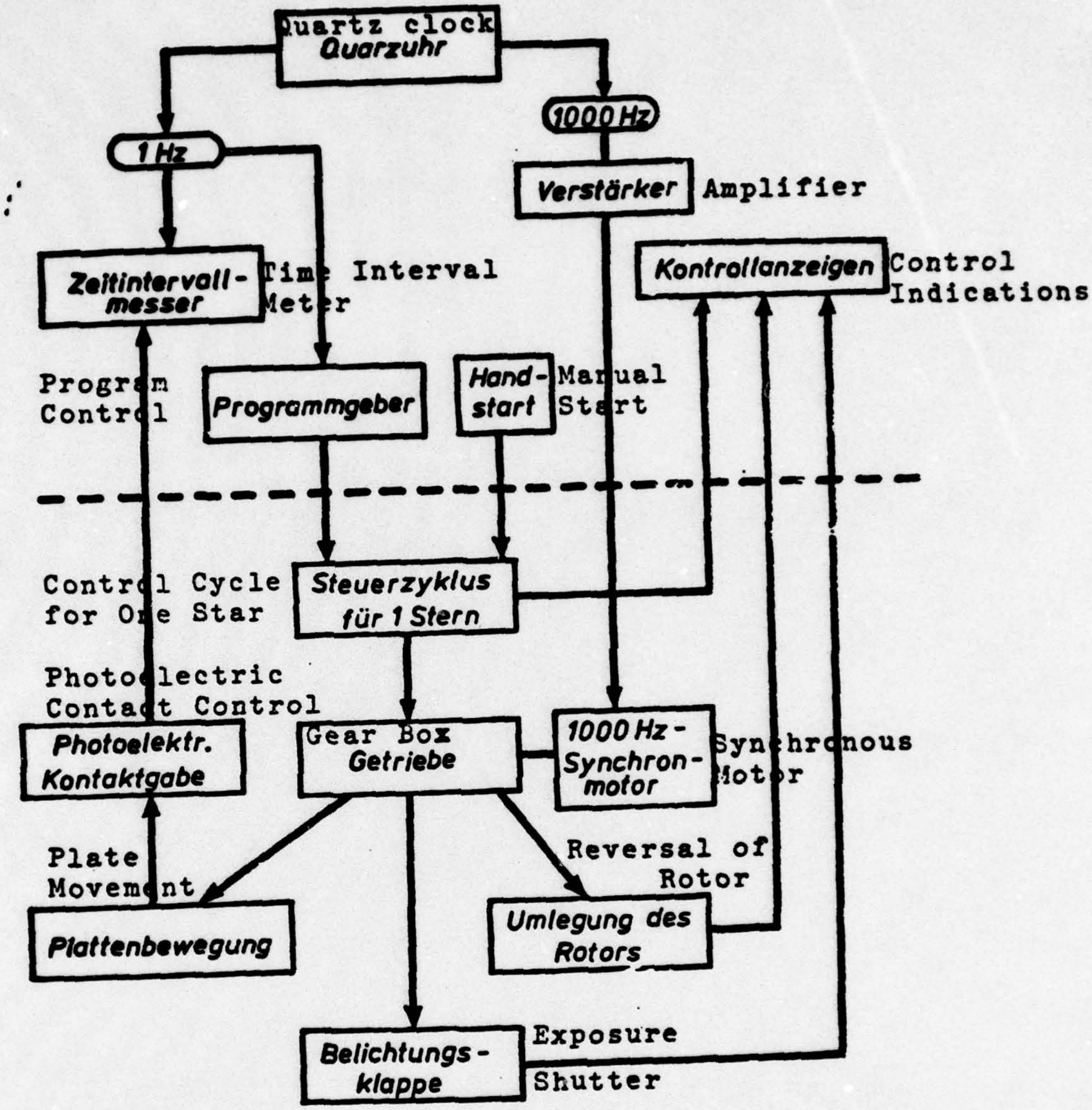

Figure 5. Functional Diagram of the PZT

positions of the follower pins 14 (Figure 4) are compensated by the opposite motion in the two positions of the instrument head. Irregular errors in the drive are equalized by time summing during the exposure.

3. THEORY OF THE EVALUATION

3.1. Fundamental Relationships Between Image Coordinates, Declination, Hour Angle and Geographic Latitude

We specify an image coordinate system, of which the y'-axis points south and the x'-axis west. A spatial rectangular coordinate system is so oriented that its positive z-axis points to the north pole, the x-axis is parallel to the x'-axis and the y-axis lies in the meridian plane.

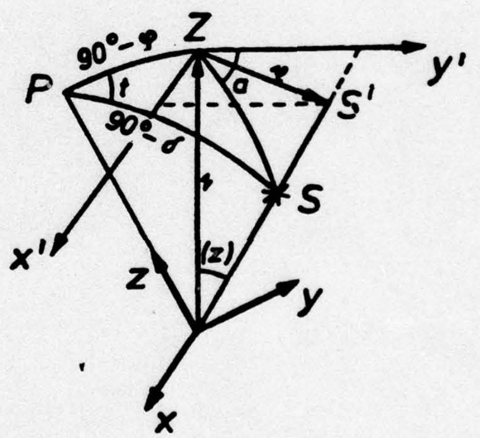

Figure 6. Image Coordinate System and Spatial Coordinate System

Figure 6 shows the relative position of the various coordinate systems. In the spatial coordinate system, the unit vector in the direction of the star becomes

$$(1) \quad s = \begin{pmatrix} \cos\delta \sin t \\ \cos\delta \cos t \\ \sin\delta \end{pmatrix} .$$

The telescope axis (imaging constant c) is illustrated by the vector

$$(2) \quad \mathfrak{c} = c \begin{bmatrix} 0 \\ \cos\varphi \\ \sin\varphi \end{bmatrix}$$

The image coordinate system is defined by the unit vectors in the direction of its coordinate axes:

$$(3) \quad \mathfrak{i}' = \begin{bmatrix} 1 \\ 0 \\ 0 \end{bmatrix}, \qquad \mathfrak{j}' = \begin{bmatrix} 0 \\ \sin\varphi \\ -\cos\varphi \end{bmatrix}.$$

The position vector of the star image in the image plane is obtained in accordance with the vectorial realtionship

$$(4) \quad \mathfrak{r} = \lambda\mathfrak{s} - \mathfrak{c},$$

wherein λ results from the scalar product

$$\mathfrak{r} \cdot \mathfrak{c} = \lambda\mathfrak{s} \cdot \mathfrak{c} - c^2 = 0$$

as

$$(5) \quad \lambda = \frac{c^2}{\mathfrak{s} \cdot \mathfrak{c}}$$

The image coordinates are obtained from (4) on the basis of the relationships

$$(6) \quad \begin{cases} x' = \mathfrak{r} \cdot \mathfrak{i}' = \lambda\mathfrak{s} \cdot \mathfrak{i}' = c^2 \dfrac{\mathfrak{s} \cdot \mathfrak{i}'}{\mathfrak{s} \cdot \mathfrak{c}}, \\[2ex] y' = \mathfrak{r} \cdot \mathfrak{j}' = \lambda\mathfrak{s} \cdot \mathfrak{j}' = c^2 \dfrac{\mathfrak{s} \cdot \mathfrak{j}'}{\mathfrak{s} \cdot \mathfrak{c}}. \end{cases}$$

In consideration of formulas (1), (2) and (3), the following relationships result from (6) between the image coordinates, the astronomical equatorial coordinates and the geographic latitude:

$$(7) \quad \begin{cases} x' = c \dfrac{\cos\delta \sin t}{\sin\varphi \sin\delta + \cos\varphi \cos\delta \cos t}, \\[2ex] y' = c \dfrac{\sin\varphi \cos\delta \cos t - \cos\varphi \sin\delta}{\sin\varphi \sin\delta + \cos\varphi \cos\delta \cos t}. \end{cases}$$

In the following, (7) will be designated as imaging equations.

3.1.1. Considerations of the Influence of Diffraction

Formula (7) represents the purely geometrical relationship between the astronomical and the image coordinates. In it, the actual pattern of the light ray, which, as is known, is curved due to astronomical refraction, is not yet taken into consideration.

In order to make it possible to consider the influence of refraction, we derive the relationships between the image coordinates and the horizon system in accordance with Figure 6. These become:

$$(8)\quad x' = f \tan z \sin a, \qquad y' = f \tan z \cos t\ .$$

In (8), f≈c is the focal distance of the PZT and z the zenith distance. It is known that the relationship between the actual zenith distance z and the zenith distance z_R, which is altered due to the refraction, is

$$(9)\quad z - z_R = r_0 \tan z,$$

wherein r_0 = 0.000 294 is the coefficient of refraction. Because only stars are observed with the PZT, which are near the zenith,

$$z \approx \tan z,$$

so that, from (9)

$$(10)\quad \tan z_R = (1 - r_0) \tan z$$

results. It follows from (10) that the relationships (8) remain valid when

$$c = (1 - r_0)\, f$$

Consequently, refraction need not be taken into consideration if the evaluation method of the PZT is so designed that c is also determined as an unknown.

Any linear proportion of the distortion of the objective, which may be present, can be compensated in the same manner. Because of the slight inclination of the principal rays with respect to the optical axis, the influence of distortion proportions of a higher order can be neglected.

3.1.2. Series Developments of the Imaging Equations

Because zenith-near stars are observed with the PZT, it is possible to introduce series developments for the angle functions of the hour angles in (7). If we set

$$\cos t = 1 - \frac{t^2}{2}, \qquad \sin t = t - \frac{t^3}{6}$$

and take into consideration that, for the meridian zenith distance

$$z_m = \varphi - \delta$$

applies, then

$$\sin\varphi\sin\delta + \cos\varphi\cos\delta = \cos z_m \approx 1 - \frac{z_m^2}{2},$$
$$\sin\varphi\cos\delta - \cos\varphi\sin\delta = \sin z_m \approx z_m - \frac{z_m^3}{6}.$$

If we now illustrate the still remaining functions of δ as functions of the geographic latitude φ and of the zenith distance z_m, the following is obtained from (7), after some elementary transformations:

$$(11)\begin{cases} x' = c\cos\varphi\, t + c\sin\varphi\, z_m t + \frac{c}{2}\cos\varphi\,(\cos^2\varphi - \frac{1}{3})\, t^3 \dots, \\ y' = c\, z_m - \frac{c}{4}\sin 2\varphi\, t^2 + \frac{c}{2}\cos 2\varphi\, z_m t^2 + \frac{c}{2} z_m^3 \dots \end{cases}$$

We want to investigate which errors develop by neglecting the terms of the third order. The following parameters apply to the Potsdam PZT:

$$\varphi = 52^\circ 24', \qquad \cos\varphi = 0{,}6101,$$
$$c = 3773\text{ mm}, \qquad \sin\varphi = 0{,}7923.$$

The maximal zenith distance, which can still be observed, amounts to

$$z_m = 15' ,$$

and an hour angle cannot exceed

$$t = 60^s$$

With these values, the following terms of the third order result:

$$\frac{c}{2} \cos\varphi \left(\cos^2\varphi - \frac{1}{3}\right) t^3 = 3{,}7 \cdot 10^{-6}\ \text{mm},$$

$$\frac{c}{2} \cos 2\varphi\, z_m\, t^2 + \frac{c}{3} z_m^3 = 1{,}4 \cdot 10^{-4}\ \text{mm} .$$

Both terms provide maximum errors, which are far below the standard deviation of the image corrdinate measurement (about plus or minus 2 μm). Further investigations can be based on the equations

$$(12)\quad x' = c \cos\varphi\, t + c \sin\varphi\, z_m\, t , \qquad y' = c\, z_m - \frac{c}{4} \sin 2\varphi\, t^2$$

3.1.3. The Modification of the Imaging Equations Resulting from the Motion of the Plate Carrier During Exposure

A static imaging process was assumed in the investigations so far. As a result of the finite exposure time and the follow-up of the plate, which is thus necessary, the imaging process is actually dynamic. This must be taken into consideration in the equations, which are the basis of the evaluation.

We introduce the following quantities for the further investigations: t_0 as the point in time of the beginning of the exposure, τ as the exposure time (time of follow-up), $t_M = t_0 + \tau/2$ as the middle of the exposure and t_m as the point in time of the meridian transit. In the following, t is the continuous time recording. With the above designations, the following results in accordance with (12):

$$(13)\quad z = \begin{bmatrix} \frac{15c}{\rho} \cos \varphi \, (t - t_m) + \frac{15c}{\rho^2} \sin \varphi \, z_m \, (t - t_m) \\ \frac{c}{\rho} z_m - \frac{c}{4} \frac{225}{\rho^2} \sin 2\varphi \, (t - t_m)^2 \end{bmatrix} .$$

It has also been taken into consideration in (13) that t is introduced in time seconds and z_m in angle seconds.

From (13), we obtain the velocity of motion of a star image in the image plane

$$(14)\quad b_s = \frac{dz}{dt} = \begin{bmatrix} \frac{15c}{\rho} \cos \varphi + \frac{15c}{\rho^2} \sin \varphi \, z_m \\ . \\ - \frac{c}{2} \frac{225}{\rho^2} \sin 2\varphi \, (t - t_m) \end{bmatrix}$$

(14) gives the speec of motion of the PZT plate carrier, which is necessary to produce a point-shaped image of the star. Because a straight-line motion in the direction of the x' axis of the image coordinate system takes place in the PZT with a speed of 15 c cos φ/ρ, strictly speaking, an a priori point-shaped image is not assured. In addition to this error influence, which is a function of the construction, it must also be taken into consideration that the direction of motion of the plate carriage can include an angle α (plate stage azimuth) with the x' axis. The actual speed of motion v_p can also deviate from the above nominal value. If we designate the velocity vector of the plate motion with

$$(15)\quad b_p = \begin{bmatrix} v_p \cos \alpha \\ -v_p \sin \alpha \end{bmatrix},$$

the necessary condition $b_s - b_p = 0$ is not fulfilled as a rule and we must expect a velocity difference

$$(16)\quad \Delta b = b_s - b_p$$

as a result of which we obtain a positional error of the centroid of the star image

$$(17)\quad \Delta\varepsilon = \frac{1}{2}\int_{t_o}^{t_o+\Delta\tau} \Delta\omega \; dt$$

With

$$\Delta\omega = \begin{bmatrix} \frac{15c}{\rho}\cos\varphi + \frac{15c}{\rho^2}\sin\varphi\, s_m - v_p\cos\alpha \\ -\frac{c}{2}\frac{225}{\rho^2}\sin 2\varphi\,(t - t_m) + v_p\sin\alpha \end{bmatrix}$$

the result is, in accordance with (17)

$$(18)\quad \Delta\varepsilon = \begin{bmatrix} \frac{15c}{\rho}\cos\varphi\,\frac{\tau}{2} + \frac{15c}{\rho^2}\sin\varphi\, s_m\frac{\tau}{2} - v_p\cos\alpha\,\frac{\tau}{2} \\ -\frac{c}{4}\frac{225}{\rho^2}\sin 2\varphi\,(t_o - t_m + \frac{\tau}{2}) + v_p\sin\alpha\,\frac{\tau}{2} \end{bmatrix} .$$

If we set

$$v_p = \frac{15c}{\rho}\cos\varphi + \Delta v ,$$

then

$$(19)\quad \Delta\varepsilon = \begin{bmatrix} \frac{15c}{\rho}\cos\varphi\,\frac{\tau}{2} + \frac{15c}{\rho^2}\sin\varphi\, s_m\frac{\tau}{2} - (\frac{15c}{\rho}\cos\varphi + \Delta v)\cos\alpha\,\frac{\tau}{2} \\ -\frac{c}{4}\frac{225}{\rho^2}\sin 2\varphi\,(t_o - t_m + \frac{\tau}{2}) + (\frac{15c}{\rho}\cos\varphi + \Delta v)\sin\alpha\,\frac{\tau}{2} \end{bmatrix} .$$

For $\Delta\varepsilon = 0$ and $\alpha = 0$, we obtain, from (19), the positional error, which is a function of the construction

$$(20)\quad \Delta\varepsilon = \begin{bmatrix} \frac{15c}{\rho^2}\sin\varphi\, s_m\frac{\tau}{2} \\ -\frac{c}{4}\frac{225}{\rho^2}\sin 2\varphi\,(t_o - t_m + \frac{\tau}{2}) \end{bmatrix} .$$

With (13), the result is, in accordance with

$$(\varepsilon) = \varepsilon_o(t_o) + \Delta\varepsilon$$

the modified imaging equation. In consideration of small angles α, we obtain for its components:

$$
(21) \quad \begin{cases} (x_0') = \frac{15c}{\rho}(t_0 - t_m) + \frac{15c}{\rho^2}\sin\varphi\,(t_M - t_m)\,z_m + \frac{15c}{4\rho^3}\cos\varphi\,\alpha^2\tau - \frac{\Delta v}{2}\tau, \\ (y_0') = \frac{c}{\rho}z_m - \frac{225}{4}\frac{c}{\rho^2}\sin 2\varphi\,(t_0 - t_m)^2 - \frac{225}{4}\frac{c}{\rho^2}\sin 2\varphi\,(t_M - t_m) + \\ \quad + \frac{15c}{2\rho^2}\alpha\tau + \frac{1}{2\rho}\tau\Delta v\alpha\,. \end{cases}
$$

The above equations are the imaging equations of the PZT with consideration of the dynamic exposure process. In order to obtain equations, which can be made the basis of the evaluation of the PZT observations, the pattern of the observation cycle must first be analyzed more closely.

3.2. The Observation Cycle

Four exposures are made in the observation of the star transit with the PZT. Between exposures, the plate is rotated by 180° (reversal). In general, the observation cycle starts when the drive motor for the plate follow-up is located to the east of meridian (position-east). In this situation, the position of the image coordinate system (positive image), which is illustrated in Figure 6, should prevail. Figure 7 shows the development of the four exposed star images in accordance with the time pattern given in Figure 2.

The first exposure (τ = 20 seconds), during which the plate stage follows up, begins 5 seconds after the initiation of the observation cycle. If, at the beginning of the exposures, zenith image and plate time ($Z = Z'$) coincide, Z' is moved into the ($Z' = Z'_I$) position as a result of the plate motion. The amount of the displacement is $15\ c \cos\varphi\ \tau/\rho$. Due to the reversal, the plate zenith reaches the position ($Z' = Z'_{II}$) and is transported into the initial position ($Z = Z'$) during the next displacement. The process is repeated in the same manner for the third and fourth exposures.

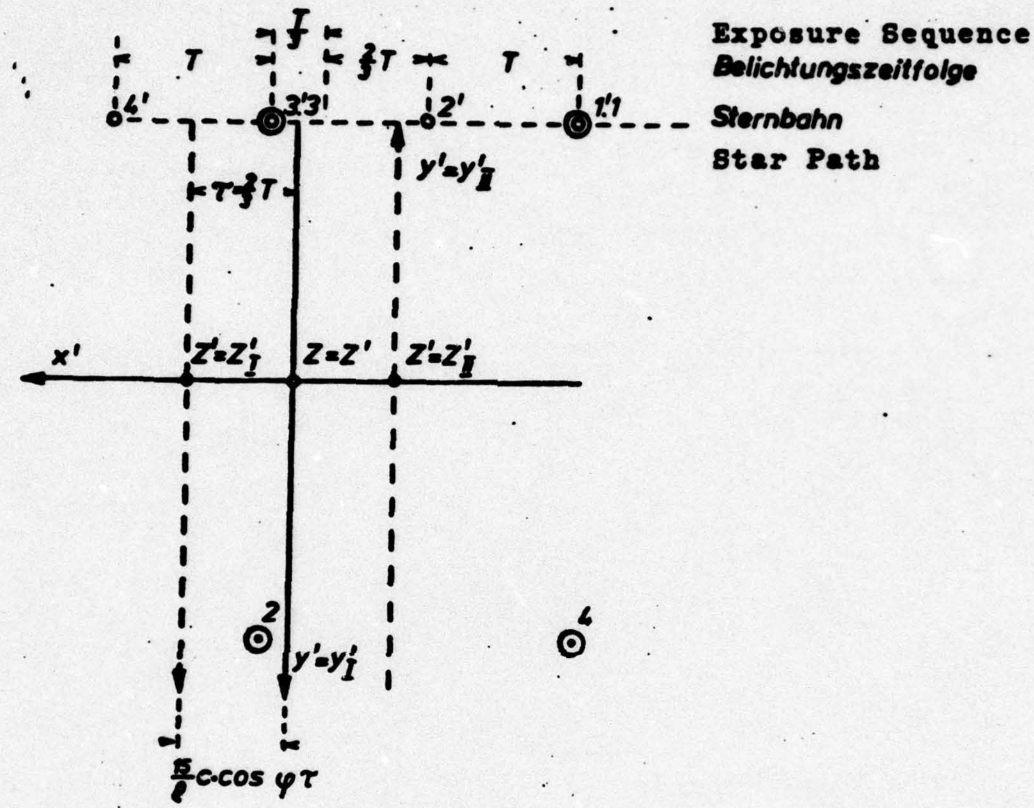

Figure 7. The Relative Position of the Star Images

The star positions (1', 2', 3', 4') in the image plane at the beginning of the exposure are illustrated in Figure 7. The exposure of positions 1' and 3' takes place in the position-east, so that their images on the photographic plate have the same position as in the image plane. The exposure of 2' and 4' takes place with the plate rotated by 180° and displaced by $15\ c \cos\varphi\ \tau h$, with the result that the photographic images are in positions 2 and 4.

If the image coordinates in the initial position (Figures 1 and 3) are designated x'_I and y'_I, then, on the basis of the

rotation and displacement of the plate,

$$(22)\quad x'_{II} = -x'_I - \frac{15c}{\rho}\cos\varphi\,\tau, \qquad y'_{II} = -y'_I.$$

The image coordinates given by (21) must be introduced in (22) for position I.

3.2.1. The Influence of the Reversal Error

In the above derivations, we had quietly assumed that the reversal takes place without error, i.e. the head of the instrument is rotated by exactly 180°. However, this assumption will not be fulfilled in practice and we must assume that the angle of rotation deviates from 180° by an amount ω (reversal error). This error influences the image coordinates in two different ways:

1. The direction of motion of the plate stage has a different azimuth error in position II than in position I. As a result, the imaging equations (21) change for this position.

2. The transformation between the image coordinates in positions I and II must be carried out with an angle of rotation $180° + \omega$.

We take the first effect of the reversal error into consideration by replacing in (21) by ($\alpha + \omega$), and the transformation between the image coordinates is carried out in accordance with the formulas

$$(23)\quad \begin{cases} x'_{II} = -(x')\cos\omega + (y')\sin\omega - \frac{15c}{\rho}\cos\varphi\,\tau = -(x') + (y')\frac{\omega}{\rho} - \frac{15c}{\rho}\cos\varphi\,\tau, \\ y'_{II} = -(y')\cos\omega - (x')\sin\omega = -(y') - (x')\frac{\omega}{\rho}. \end{cases}$$

An investigation of the order of magnitude of the coefficients of α and ω shows that it is possible to limit to linear terms in our imaging equations because of the small values of these angles. With consideration of (22) and (23), the following imaging equations result from (21):

$$
(24)\quad \begin{cases}
x'_I = \frac{15c}{\rho}\cos\varphi\,(t_o - t_m) + \frac{15c}{\rho^2}\sin\varphi\,(t_M - t_m)\,z_m - \frac{\tau}{2}\,\Delta v\,, \\
y'_I = \frac{c}{\rho}\,z_m - \frac{225}{4}\frac{c}{\rho^2}\sin 2\varphi\,(t_o - t_m)^2 - \frac{225}{4}\frac{c}{\rho^2}\sin 2\varphi\,(t_M - t_m)\tau + \\
\qquad + \frac{15c}{2\rho^2}\cos\varphi\,\tau\,\alpha\,, \\
x'_{II} = \frac{15c}{\rho}\cos\varphi\,(t_o - t_m) - \frac{15c}{\rho^2}\sin\varphi\,(t_M - t_m)\,z_m + \frac{\tau}{2}\,\Delta v + \frac{c}{\rho^2}\,z_m\,\omega - \\
\qquad - \frac{15c}{\rho}\cos\varphi\,\tau\,, \\
y'_{II} = -\frac{c}{\rho}\,z_m + \frac{225}{4}\frac{c}{\rho^2}\sin 2\varphi\,(t_o - t_m)^2 + \frac{225}{4}\frac{c}{\rho^2}\sin 2\varphi\,(t_M - t_m)\,\tau - \\
\qquad - \frac{15c}{2\rho^2}\cos\varphi\,\tau\,\alpha - \frac{15c}{\rho^2}\cos\varphi\,(t_o - t_m)\,\omega\,.
\end{cases}
$$

In (24), we introduce the following designations for the coefficients, which are a function of the location and of the construction of the PZT:

$$
(25)\quad \begin{cases}
a_x = \frac{15c}{\rho}\cos\varphi\,, \qquad b_x = \frac{15c}{\rho^2}\sin\varphi\,, \\
a_y = \frac{c}{\rho}\,, \qquad b_y = \frac{225}{4}\frac{c}{\rho^2}\sin 2\varphi\,.
\end{cases}
$$

Thus, the following form of the imaging equations is obtained from (24):

$$
(26)\quad \begin{cases}
x'_I = a_x\,(t_o - t_m) + b_x\,(t_M - t_m)\,z_m - \frac{\tau}{2}\,\Delta v\,, \\
y'_I = a_y\,z_m - b_y\left\{(t_o - t_m)^2 + (t_M - t_m)\,\tau\right\} + \frac{a_x}{2\rho}\,\tau\,\alpha\,, \\
x'_{II} = -a_x\,(t_o - t_m) - b_x\,(t_M - t_m)\,z_m + \frac{\tau}{2}\,\Delta v + \frac{a_y}{\rho}\,z_m\,\omega - a_x\tau\,, \\
y'_{II} = -a_y\,z_m + b_y\left\{(t_o - t_m)^2 + (t_M - t_m)\,\tau\right\} - \frac{a_x}{2\rho}\,\tau\,\alpha - \frac{a_x}{\rho}\,(t_o - t_m)\,\omega\,.
\end{cases}
$$

3.3. The Relationships Between the Coordinate System of the Evaluation Apparatus and the Image Coordinate System

The evaluation of the PZT plates is carried out in the Geodetic-Astronomical Observatory Potsdam, using the coordinate measuring apparatus "Ascorecord" of VEB Carl Zeiss Jena. In this manner, coordinate values in the system of the measuring apparatus result. The measurement is carried out on the exposed negative plates of the PZT observation.

For a closed form of the evaluation, it is appropriate to form the imaging relationship between measured coordinates - in the system of the coordinate measuring apparatus - and the spherical values z_m and t_m. Figure 8 illustrates the relationships between the coordinate systems of the positive image, of the negative image and of the coordinate measuring apparatus.

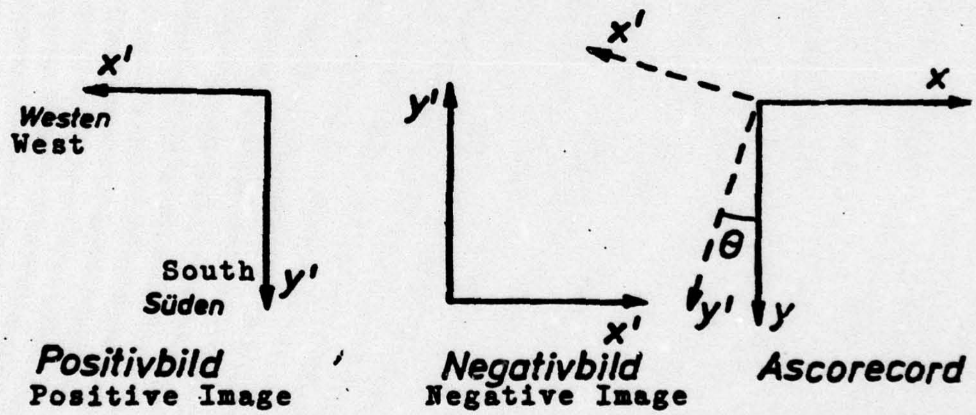

Figure 8. The Relative Position of the Coordinate Systems of the Positive Image, of the Negative Image and of the Coordinate Measuring Apparatus

If we now still take into consideration that, generally, an orientation error θ exists between the image coordinate system and the apparatus coordinate system, the following transformation equations are easily read from Figure 8:

$$(27)\quad y' = y\cos\theta - x\sin\theta + y_0\,, \qquad x' = -x\cos\theta - y\sin\theta + x_0\,.$$

3.4. Derivation of the Fundamental Formula for the Evaluation

The determination of the geographic latitude and time correction is carried out in accordance with formulas

$$(28) \quad \varphi = \delta + z_m, \qquad \Delta U = k\left(\alpha - \lambda - SZ_{0_{Gr}}\right) - t_m + 0\overset{s}{,}021\,;$$

where δ is the declination, α the right ascension, λ the geographic longitude, $SZ_{0_{Gr}}$ the star time for zero hours earth time, $k = 0.997\ 269\ 57$ is the conversion factor of star time intervals into intervals of mean time and 0.021 second is the correction as a consequence of daily aberration. z_m and t_m are used in the derived imaging equations and must be determined in the evaluation process.

In addition, we had established in Section 3.1.1. that it is necessary, for the purpose of excluding the proportion of the astronomical refraction, which is constant during the observation, to determine the imaging constant c in the evaluation process. c is contained in the coefficient a_x (scale factor) in the system of formulas (26); we want to introduce it as a further unknown in the evaluation.

A priori, the transformation relationship (27) is also unknown to us. However, we wish to give its constant only in so far as it is necessary for the evaluation process.

Because of the structure of the matrix resulting from the imaging equations for a star transit, ω and φ cannot be determined in the evaluation process, but only by additional measuring means or especially arranged observation processes. As the observation values, the measured image coordinates (x_i, y_i) and -- at least in fractions of a second -- the registered time of the middle of the observation cycle are the basis of the evaluation process.

3.4.1. The Imaging Equations for a Star Transit

During a star transit, exposures of images 1 and 3 take place in position I and images 2 and 4 in position II. If this is taken into consideration, the following imaging equations are obtained for the four images of a star transit:

$$
\text{(29a)} \quad \left\{
\begin{aligned}
x_0 - x_1 \cos\theta - y_1 \sin\theta &= a_x (t_1 - t_m) + b_x z_m (t_{M_1} - t_m) - \tfrac{T}{2}\Delta v\,, \\
x_0 - x_2 \cos\theta - y_2 \sin\theta &= -a_x (t_2 - t_m) - b_x z_m (t_{M_2} - t_m) + \tfrac{T}{2}\Delta v + \\
&\quad + \frac{a_y}{\rho} z_m \omega - a_x \tau\,, \\
x_0 - x_3 \cos\theta - y_3 \sin\theta &= a_x (t_3 - t_m) + b_x z_m (t_{M_3} - t_m) - \tfrac{T}{2}\Delta v\,, \\
x_0 - x_4 \cos\theta - y_4 \sin\theta &= -a_x (t_4 - t_m) - b_x z_m (t_{M_4} - t_m) + \tfrac{T}{2}\Delta v + \\
&\quad + \frac{a_y}{\rho} z_m \omega - a_x \tau\,,
\end{aligned}
\right.
$$

$$
\text{(29b)} \quad \left\{
\begin{aligned}
y_0 + y_1 \cos\theta - x_1 \sin\theta &= a_y z_m - b_y \left\{(t_1 - t_m)^2 + (t_{M_1} - t_m)\tau\right\} + \\
&\quad + \frac{a_x}{2\rho}\tau\alpha\,, \\
y_0 + y_2 \cos\theta - x_2 \sin\theta &= -a_y z_m + b_y \left\{(t_2 - t_m)^2 + (t_{M_2} - t_m)\tau\right\} - \\
&\quad - \frac{a_x}{2\rho}\tau\alpha - \frac{a_x}{\rho}(t_2 - t_m)\omega\,, \\
y_0 + y_3 \cos\theta - x_3 \sin\theta &= a_y z_m - b_y \left\{(t_3 - t_m)^2 + (t_{M_3} - t_m)\tau\right\} + \\
&\quad + \frac{a_x}{2\rho}\tau\alpha\,, \\
y_0 + y_4 \cos\theta - x_4 \sin\theta &= -a_y z_m + b_y \left\{(t_4 - t_m)^2 + (t_{M_4} - t_m)\tau\right\} - \\
&\quad - \frac{a_x}{2\rho}\tau\alpha - \frac{a_x}{\rho}(t_4 - t_m)\omega\,.
\end{aligned}
\right.
$$

In the above equations, the points in time of the beginning of the exposures were designated as t_1, t_2, t_3, t_4 and the time of the mean exposures as t_{M1}, t_{M2}, t_{M3}, t_{M4}. The exposures take place in intervals of $T = 30$ seconds, so that the following relationships can be taken into consideration in the following derivations:

$$
(30)\quad
\begin{aligned}
t_2 &= t_1 + T, & t_{M_2} &= t_{M_1} + T, \\
t_3 &= t_1 + 2T, & t_{M_3} &= t_{M_1} + 2T, \\
t_4 &= t_1 + 3T, & t_{M_4} &= t_{M_1} + 3T
\end{aligned}
$$

3.4.2. Orientation Unknown θ and Scale Factor a_x

The calculation of the orientation unknown is carried out with the aid of the system of equations (29b). By appropriate subtraction and addition, the following equation is obtained:

$$
(31)\quad (y_4 - y_2 + y_1 - y_3)\cos\theta - (x_4 - x_2 + x_1 - x_3)\sin\theta =
$$
$$
= b_y \cdot \left\{ (t_4 - t_m)^2 - (t_2 - t_m)^2 + (t_3 - t_m)^2 - (t_1 - t_m)^2 + \right.
$$
$$
\left. + (t_{M_4} - t_{M_2} + t_{M_3} - t_{M_1})\tau \right\} - \frac{a_x}{\rho}(t_4 - t_2)\omega .
$$

The term multiplied by b_y in the above formula can be brought into the following form, with consideration of (30):

$$
(t_4 - t_m)^2 - (t_2 - t_m)^2 + (t_3 - t_m)^2 - (t_1 - t_m)^2 + (t_{M_4} - t_{M_2} + t_{M_3} - t_{M_1})\tau =
$$
$$
= 2T\,(t_1 + t_2 + t_3 + t_4 - 4t_m + 2\tau) .
$$

On the basis of the system of equations (29b), this time expression can be illustrated as a function of the image coordinates. With

$$
(32)\quad t_s = t_1 + t_2 + t_3 + t_4
$$

the result is

$$
t_s - 4t_m + 2\tau = \frac{1}{a_x + b_x a_m}\left\{ (x_2 - x_1 + x_4 - x_3)\cos\theta + (y_2 - y_1 + y_4 - y_3)\sin\theta \right\}.
$$

If we insert this in (31) and consider the relationships

$$(33)\begin{cases} y_a = y_1 - y_2 - y_3 + y_4\,, & x_a = x_1 - x_2 - x_3 + x_4\,, \\ y_t = -y_1 + y_2 - y_3 + y_4\,, & x_t = -x_1 + x_2 - x_3 + x_4\,, \end{cases}$$

we obtain the following formula for the determination of the orientation unknown:

$$(34)\quad \tan\theta = \frac{y_a}{x_a} - \frac{2T\,b_y}{a_x + b_x(z_m)}\left(\frac{x_t}{x_a} + \frac{y_t\,y_a}{x_a^2}\right) + \frac{2a_x}{\rho}\frac{T}{x_a}w\,.$$

The values a_x, b_x, b_y and z_m, which are used in the above formula, are sufficiently accurately calculated on the basis of the approximately known geographical latitude, the focal distance and the declination of the star.

For the purpose of determining the scale factor, we form, from (29a), the expression

$$(x_1 - x_3 - x_2 + x_4)\cos\theta + (y_1 - y_3 - y_2 + y_4)\sin\theta =$$
$$= a_x(t_3 - t_1 + t_4 - t_2) + b_x z_m (t_{M_3} - t_{M_1} + t_{M_4} - t_{M_2})\,.$$

Under consideration of (30) and (33),

$$(35)\quad a_x = \frac{1}{4T}(x_a\cos\theta + y_a\sin\theta) - b_x(z_m)\,.$$

From (35), we obtain the scale factor, which is necessary for the calculation of the latitude

$$(36)\quad a_y = \frac{a_x}{15\cos\varphi}$$

and the imaging constant

$$(37)\quad c = a_y\rho = \frac{a_x}{15\cos\varphi}\rho\,.$$

3.4.3. Time and Zenith Distance of the Meridian Transit

The meridian transit time is obtained from (29a) under consideration of (30), (32) and (33) as

$$(38)\quad t_m = \frac{1}{4} t_s + \frac{\tau}{2} - \frac{x_t \cos\theta + y_t \sin\theta}{4\,(a_x + b_x(z_m))} - \frac{1}{2}\,\frac{\tau\,\Delta v}{a_x + b_x(z_m)} - \frac{1}{2}\,\frac{a_y\,(z_m)}{a_x + b_x(z_m)}\,\frac{\omega}{\rho}\ .$$

In the above formula, $1/4\ t_s + \tau/2$ is the middle of the time of the observation cycle. This value is obtained as the mean of the time recordings during the four exposure processes.

For the calculation of the zenith distance, the following equation is derived from (29b), under consideration of (33):

$$(39)\quad -y_t \cos\theta + x_t \sin\theta = 4a_y\, z_m - b_y \Big\{(t_1 - t_m)^2 + (t_2 - t_m)^2 + (t_3 - t_m)^2 + (t_4 - t_m)^2 + \tau\,(t_{M_1} + t_{M_2} + t_{M_3} + t_{M_4} - 4t_m)\Big\} + \frac{2a_x}{\rho}\,\tau\alpha + \frac{a_x}{\rho}\,(t_2 - t_4 - 2t_m)\,\omega$$

For the calculation of the bracketed expression, which is multiplied by b_y, all exposure times, except t_1, are illustrated by the relationships (30). In addition to the known values T and τ, only the difference $t_1 - t_m$ is contained in the transformed expression. Because b_y is a small value, we can, in the calculation of this difference, neglect the small angle θ and the terms in the system of equations (29), which can be ascribed to the curvature of the parallel. Then, approximately

$$t_1 - t_m = \frac{1}{a_x}\,(x_o - x_1).$$

The summation of equations (29a) results in

$$x_o = \frac{1}{4}\,(x_1 + x_2 + x_3 + x_4) - \frac{1}{2}\,T\,a_x\ ,$$

with which we obtain

$$t_1 - t_m = \frac{1}{a_x}\left(\frac{x_1 + x_2 + x_3 + x_4}{4} - x_1\right) - \frac{T}{2}$$

For the purpose of simplification, we set

$$(40)\quad t_1 - t_m = -\frac{3}{2} T + \Delta t,$$

wherein

$$(41)\quad \Delta t = \frac{1}{a_x}\left(\frac{x_1 + x_2 + x_3 + x_4}{4} - x_1\right) + T$$

If the above train of thought is taken into consideration in (39), the result is for the zenith distance

$$(42)\quad z_m = \frac{1}{4a_y}(-y_t \cos\theta + x_t \sin\theta) + \frac{b_y}{4a_y}(5T^2 + 2\tau^2 + 4\tau\Delta t + 4\Delta t^2) -$$

$$- \frac{1}{2}\frac{a_x}{a_y}\frac{\tau}{\rho}\alpha - \frac{1}{4\rho}\frac{a_x}{a_y}(t_2 + t_4 - 2t_m)\,\omega .$$

3.5. The Formulas of the Arithmetical Program of the PZT Evaluation

The formulas derived in Section 3.4 form the basis for the establishment of the arithmetic program. In them, the influences of azimuth and reversal errors are also taken into consideration. As results from the theoretical error investigations, which will still be illustrated, the errors of these values influence the result to only a slight degree, so that the required tolerances of azimuth and reversal are easily maintained and $\omega = 0$ and $\alpha = 0$ can be assumed for the evaluation. The same assumption is also justified for the error of the follow-up speed.

The definitive formulas, illustrated in the following description of the arithmetic process, apply especially to the location of the Potsdam PZT. The following values were the basis of the calculation of the constants:

$$(\varphi) = 52^\circ 24' 24'', \qquad c = 3773{,}5\ \text{mm}, \qquad T = 30^s_{MZ} = 30{,}082\,137^s_{SZ},$$
$$\tau = 20^s.$$

The programmed calculation serves, in each case, for the evaluation of a group of about 10 to 12 stars, of which the images

are located on a plate. By means of measuring the image coordinates, we obtain, for each star, the coordinates

$$x_1,\ x_2,\ x_3,\ x_4; \qquad y_1,\ y_2,\ y_3,\ y_4.$$

During the observation, the difference between the time mean of the observation cycle and the second signal of the Potsdam electronic time servide

$$dt_U = Z\ (PZT) - UTC\ (ZIPE)$$

is recorded. For a group, the mean from the recordings of all star transits is always introduced into the evaluation.

On the basis of the approximate value ( ) of the geographic latitude, an approximate value of the meridian zenith distance is calculated for each star

$$(z_m) = (\varphi) - \delta$$

From the image coordinates of each star, the values

$$y_a = y_1 - y_2 - y_3 + y_4, \qquad x_a = x_1 - x_2 - x_3 + x_4;$$

$$y_t = -y_1 + y_2 - y_3 + y_4, \qquad x_t = -x_1 + x_2 - x_3 + x_4.$$

result. With the above expressions, the prientation unknown is obtained in accordance with (34)

$$\tan\theta = \frac{y_a}{x_a} - \frac{2T\ b_y}{a_x + b_x(z_m)}\left(\frac{x_t}{x_a} + \frac{y_t\ y_a}{x_a^2}\right) = \frac{y_a}{x_a} - 0{,}001\ 733\ 2\left(\frac{x_t}{x_a} + \frac{y_t\ y_a}{x_a^2}\right).$$

From all values θ, which result for a group, the arithmetic mean is formed and introduced in the further evaluation.

In accordance with (35), the scale factor

$$a_x = \frac{1}{2T}(x_a \cos\theta + y_a \sin\theta) - b_x(z_m) =$$

$$= 0{,}831\ 057\ 9 \cdot 10^{-2}\ (x_a \cos\theta + y_a \sin\theta) - 0{,}105\ 471 \cdot 10^{-5}(z_m).$$

results, for which the mean of all values of the group is also formed and introduced into the further evaluation. For the calculation of the meridian distances, we form the value

$$a_y = \frac{a_x}{15 \cos \varphi} = \frac{a_x}{9{,}150\,778\,5}$$

and

$$e = 206\,264{,}81\, a_y .$$

from the above formula.

In order to determine the time correction, we first calculate the earth time of the meridian transit for all stars. If all values are introduced in seconds, the result is

$$t_o = (\alpha - \lambda - SZ_{o,Gr}) \cdot 0{,}997\,269\,57,$$

wherein α is the right ascension, λ the geographic longitude and $SZ_{0,Gr}$ the star time for zero hours earth time. In accordance with (38), we calculate

$$t_m = -\frac{1}{4\,(a_x + b_x(z_m))} \left\{x_t \cos\theta + y_t \sin\theta\right\} =$$

$$= -\frac{0{,}997\,269\,57}{4\,(a_x + 0{,}105\,471 \cdot 10^{-5}(z_m))} \left\{x_t \cos\theta + y_t \sin\theta\right\} .$$

We thus obtain the time correction as

$$dU = (t_o + 0^s_{,}021 - t_m + dt_U).$$

Of the above value, only the fractions of seconds are usable, because the mean of the observation cycle is established only with respect to these fractions.

For the determination of the zenith distance, the value

$$\Delta t = \frac{1}{a_x} \left\{\frac{x_1 + x_2 + x_3 + x_4}{4} - x_1\right\} + T =$$

$$= 5{,}973 \left\{\frac{x_1 + x_2 + x_3 + x_4}{4} - x_1\right\} + 30^s$$

is first calculated, with which we obtain the zenith distance

$$z_m = \frac{1}{4a_y}(-y_t \cos\theta + x_t \sin\theta) + \frac{b_y}{4a_y}(5T^2 + 2\tau^2 + 4\tau\Delta t + 4\,\Delta t^2) =$$

$$= \frac{1}{4a_y}(-y_t \cos\theta + x_t \sin\theta) + 0{,}35'' + 0{,}003\,29\,\Delta t + 0{,}000\,264\,\Delta t^2$$

On the basis of the zenith distances, a value of geographic latitude

$$\varphi = \delta + z_m.$$

results.

A mean value of the geographic latitude and of the time correction is calculated for each group. In accordance with known formulas of error theory, the program is supplemented by calculations of the mean errors of the individual and mean values for θ, a_x, dU and φ.

4. THEORETICAL ERROR CONSIDERATIONS

4.1. The Influence of Azimuth and Reversal Errors on Time Correction and Zenith Distance

Let us assume that the orientation unknown is influenced only by the reversal error and let us apply formula (34) for this case, then we directly obtain the error of the orientation unknown, which is caused by ω

$$d\Theta = 2a_x \frac{T}{x_m} \omega .$$

With this value, the error of the time correction results from (39)

$$(43) \quad dt_m = -\frac{1}{2} \left\{ \frac{y_t}{(a_x + b_x z_m)} \frac{a_x T}{x_m} + \frac{a_y z_m}{(a_x + b_x z_m)} \right\} \frac{\omega}{\rho} .$$

From formulas (29),

$$x_m = 4a_x T, \qquad y_t = -4a_y z_m$$

is approximately obtained, where the factor of ω/ρ disappears in (43). In the first order, a reversal error therefore has no influence on the determination of the time correction. The influence of the azimuth error also disappears. From (42),

$$dz_m = \frac{x_t}{4a_y} \frac{d\Theta}{\rho} - \frac{1}{4\rho} \frac{a_x}{a_y} (t_2 + t_4 - 2t_m) \omega .$$

is obtained for the influence of the reversal error on the zenith distance.

If the influence of the reversal error on the orientation unknown is taken into consideration in the above formula, and if, as an approximation,

$$x_t = a_x (t_1 + t_2 + t_3 + t_4 - 4t_m),$$

is used, the result is, for the influence of the reversal

error on the zenith distance

$$(44)\quad dz_{m_\omega} = -\frac{1}{4}\frac{a_x}{a_y}T\frac{\omega}{\rho}\ .$$

The influence of an azimuth error on the zenith distance can be read directly from (42):

$$(45)\quad dz_{m_\alpha} = -\frac{1}{2}\frac{a_x}{a_y}\frac{T}{\rho}\alpha\ .$$

If we insert the values for a_x, a_y, T and ,resultinf from the construction parameters and the location of the PZT, in (44) and (45), then

$$(46)\quad dz_{m_\omega} = -3{,}33\cdot 10^{-4}\omega\ ,$$

$$(47)\quad dz_{m_\alpha} = 4{,}44\cdot 10^{-4}\alpha\ .$$

If we admit an error of 0.01", caused by both influences, in the zènith distance, then

$$\omega \leq 30'' \quad \text{and} \quad \alpha \leq 20''$$

The influences of systematic error proportions of α and ω are illustrated by (43), (44) and (45). An irregular change in the azimuth error in the course of the observation cycle cannot be expected. In comparison, we can assume that the reversal error changes by irregular amounts after each change in postition. The influence of irregular changes of the reversal error is obtained by the assumption of different values of ω for each position of the observation cycle. This is taken into consideration in formulas (29) and the error propagation law is applied to (38) and (42). The following is obtained

$$(48)\quad m_{t_{m,\omega}} = 0{,}3\frac{a_y}{a_x}\frac{s_m}{\rho}m_\omega$$

and

$$(49)\quad m_{z_{m,\omega}} = \frac{0{.}517}{\rho}\frac{a_x}{a_y}m_\omega\ .$$

If the values a_x, a_y are inserted and the maximal possible zenith distance $z_m = 15'$ is assumed, the result is

$$m_{t_{m,\omega}} = 1{,}45\cdot10^{-4}\, m_\omega \,, \qquad m_{z_{m,\omega}} = 6{,}9\cdot10^{-4}\, m_\omega \,.$$

The above values show that even relatively large irregular changes of ω have only an insignificant influence on the determination of meridian zenith distance and meridian transit time.

4.2. The Theoretical Error Relationship Between the Image Coordinates and the Determined Values of z_m and t_m

It is assumed that the image coordinates are subject to only random errors and that the evaluation is carried out in accordance with the formulas summarized in Section 3.5. As the weighting unit error, the mean error of the coordinates is assumed, which has the same magnitude for both coordinate values. We thus obtain the weighting coefficients

$$Q_{xx} = Q_{yy} = 1.$$

With these values, the weighting and correlation coefficients of the values x_a, y_a, x_t and y_t result in accordance with (33)

$$(50)\quad \left\{\begin{array}{llll} Q_{y_a y_a} = 4, & Q_{y_a x_a} = 0, & Q_{y_a y_t} = 0, & Q_{y_a x_t} = 0, \\ & Q_{x_a x_a} = 4, & Q_{x_a y_t} = 0, & Q_{x_a x_t} = 0, \\ & & Q_{y_t y_t} = 4, & Q_{y_t x_t} = 0, \\ & & & Q_{x_t x_t} = 4. \end{array}\right.$$

Through the formation of the differenctial of (34), we obtain

$$(51)\quad d\vartheta = \frac{\cos^2\vartheta}{x_a}\, dy_a - y_a \frac{\cos^2\vartheta}{x_a^2}\, dx_a.$$

In the above formula, and also in those which are still to be derived, we can limit ourselves to the principal terms because the error influence of the image coordinates on the correction terms is meaningless. We want to assume that the observation is made symmetrical to the meridian, so that we can set

$$y_1 = y_3, \qquad x_1 = x_4; \qquad y_2 = y_4, \qquad x_2 = x_3$$

From this follows

$$y_a = 0, \qquad x_a = 2\,(x_1 - x_2); \qquad y_t = 2\,(y_2 - y_1), \qquad x_t = 0.$$

In addition, approximately

$$\cos\theta \approx 1, \qquad \sin\theta \approx 0.$$

In this manner, (51) becomes

$$d\theta = \frac{1}{2}\,\frac{1}{x_1 - x_2}\,dy_a\,,$$

from which the following weighting and correction coefficients are obtained:

$$(52)\quad \begin{cases} Q_{\theta\theta} = \frac{1}{4}\,\frac{1}{(x_1 - x_2)^2}\,Q_{y_a y_a} = \frac{1}{(x_1 - x_2)^2}\,, \\ Q_{\theta x_a} = 0; \qquad Q_{\theta y_a} = \frac{1}{2}\,\frac{1}{x_1 - x_2}\,Q_{y_a y_a} = \frac{2}{x_1 - x_2}\,; \\ Q_{\theta x_t} = 0; \qquad Q_{\theta y_t} = 0. \end{cases}$$

From (35), the result is

$$(53)\quad da_x = \frac{1}{4T}\,dx_a$$

or

$$(54)\quad Q_{a_x a_x} = \frac{1}{16T^2}\,Q_{x_a x_a} = \frac{1}{4T^2}\,.$$

After the calculation of θ and a_x, the group means of these values are introduced into the further evaluation. For a group of n stars, the following weighting and correlation coefficients thus result:

$$
(55)\quad
\begin{cases}
Q_{\theta\theta} = \frac{1}{n}\frac{1}{(x_1 - x_2)^2}, & Q_{\theta y_a} = \frac{1}{n}\frac{2}{x_1 - x_2}, \\
Q_{a_x a_x} = \frac{1}{4n\,T^2}, & Q_{a_x x_a} = \frac{1}{nT}, \\
Q_{a_x y_a} = 0, & Q_{a_x x_t} = 0, \qquad Q_{a_x y_t} = 0.
\end{cases}
$$

In addition,

$$
(56)\quad Q_{a_y a_y} = \frac{Q_{a_x a_x}}{15^2 \cos^2\varphi}.
$$

From the formula for the calculation of the meridian transit time (38)

$$
(57)\quad dt_m = -\frac{1}{4\,(a_x + b_x\,z_m)}\,(dx_t + y_t\,d\theta)
$$

is obtained, from which

$$
(58)\quad Q_{t_m t_m} = \frac{1}{16\,(a_x + b_x\,z_m)^2}\,(Q_{x_t x_t} + y_t^2\,Q_{\theta\theta})
$$

follows for the weighting coefficient. After some elementary transformations,

$$
(59)\quad Q_{t_m t_m} = \frac{T^2}{(x_1 - x_2)^2}\,\left(1 + \frac{1}{n}\,\frac{(y_1 - y_2)^2}{(x_1 - x_2)^2}\right).
$$

results from (58).

In the same manner,

$$
(60)\quad Q_{z_m z_m} = \frac{1}{4a_y^2}\,\left(1 + \frac{1}{900\,n\,T^2\cos^2\varphi}\,\frac{(y_2 - y_1)^2}{a_y^2}\right).
$$

is obtained from (42).

With the parameters of the PZT, the following numerical values for the weighting coefficients result for a group of n = 10 stars:

$$Q_{\theta\theta} = 10^{-3},$$

$$Q_{a_x a_x} = 2{,}78 \cdot 10^{-5}, \qquad Q_{a_y a_y} = 3{,}33 \cdot 10^{-7},$$

$$Q_{t_m t_m} = 9\,(1 + 10^{-3}\,(y_2 - y_1)^2),$$

$$Q_{z_m z_m} = 0{,}74 \cdot 10^3\,(1 + 0{,}246 \cdot 10^{-3}\,(y_2 - y_1)^2).$$

In the PZT, the maximal value of the ordinate difference amounts to $(y_2 - y_1)_{max} \approx 30$ mm, whereby the weighting coefficients of t_m and z_m fluctuate within the following range:

1. $y_2 - y_1 \approx 0, \qquad Q_{t_m t_m} = 9, \qquad Q_{z_m z_m} = 0{,}74 \cdot 10^3,$

2. $y_2 - y_1 \approx 30, \qquad Q_{t_m t_m} = 17, \qquad Q_{z_m z_m} = 0{,}90 \cdot 10^3.$

In the *coordinate measurement* with the "Ascorecord", a mean error of $m_0 \pm 0.0015$ mm is obtained, from which the mean errors of the zenith distance and of the meridian transit time

1. $m_{t_m} = \pm 0\overset{s}{,}0045, \qquad m_{z_m} = \pm 0\overset{''}{,}041,$

2. $m_{t_m} = \pm 0\overset{s}{,}0062, \qquad m_{z_m} = \pm 0\overset{''}{,}045$

are obtained.

These mean errors represent the influence of the coordinate measurement. As a rule, they will be significantly smaller than can actually be obtained with the PZT. In addition to the measuring errors, error influences must also be expected, which can be found in the distortions in the photographic emulsion and in the variations in the geometry of the imaging process through changes in the refraction influence. As will be shown later, the mean error of the image coordinates can be estimated as

$$m_0 = \pm 0{,}006 \text{ mm}$$

under consideration of all apparent conditions. With this value, the following mean errors of t_m and z_m result:

$$1.\quad m_{t_m} = \pm 0^s\!.0180, \qquad m_{z_m} = \pm 0''\!.16,$$

$$2.\quad m_{t_m} = \pm 0^s\!.0247, \qquad m_{z_m} = \pm 0''\!.18.$$

5. OBSERVATION PROGRAM

The star program for the observation with the PZT consists of a total of 257 stars up to a brightness of $9^m\!.5$ from the catalog of the Astronomical Society AGK (7). 24 groups are formed of the total number of stars. In order to keep the influence of an error in the plate scale small in the calculation of the geographical latitude, the stars of a group were so selected that the sum of their zenith distances is as small as possible. For a group of 10 stars, the plate scale can, on the average, be determined with a relative accuracy of about 1×10^{-4}. So that errors greater than $0''\!.02$ cannot develop in the latitude, the zenith distances z of the H principal stars of a group must fulfill the condition

$$(61) \quad \frac{1}{H}\left|\Sigma z\right| \leq 3'$$

The shortest time difference of two successive stars is instrumentally a function of the duration of 120 seconds for the observation cycle of one star. In some cases, the program contains stars with very small right ascension differences ($\Delta\alpha \leq 14^s$), which can be recorded with the same observation cycle.

For each group, Table 1 gives the total number of the stars, the number H of the pricipal stars, the number Z of the secondary stars, the right ascension area α and the observation period. The average number of principal stars per group amounts to 10 (minimum 8, maximum 12). If possible, three groups of stars are observed during each clear night. In the normal case, only one group is recorded on one plate. Figure

9 shows the program sequence in the course of one year. The program change takes place half-monthly by the principle of the chain method. Thus, each group is observed in a period of 1-1/2 months and the combination of two adjacent groups for one month.

The average loci and the characteristic motions of the PZT stars are summarized in the star catalog for the Potsdam PZT (4). The right ascensions and declinations were corrected on the basis of the results of the PZT observations of 1972 and 1973. The determination of the star coordinate corrections was carried out in two steps:

1. Individual corrections were derived from the residual er errors of the groups. In connection with this, the reduction of incomplete groups to the corresponding group center was carried out.

2. By the principle of the chain method, the group corrections were calculated from the differences between the groups observed during the same night.

The determination of the star coordinate corrections from the Potsdam PZT observations is illustrated in detail in (4). As an average, the accuracy for the total corrections, composed of individual and group corrections, amounts to $\pm 0\rlap{.}''08$ for the declination and $\pm 0\rlap{.}^{s}010$ for the right ascension.

Together with five additional catalogs, observed at various times since 1915, the declinations obtained from the PZT observations were used to calculate new characteristic motion components in declination for the PZT stars. As an average, the mean errors of these newly calculated characteristic motions, with $\pm 0\rlap{.}''004$, are only half as great as those of the characteristic motions of the AGK 3.

Table 1. Number Stars and Observation Periods of Groups

Group	N	H	Z	α	Observation Period
1	12	10	2	0^h02^m – 0^h46^m	1. Okt. – 15. Nov.
2	12	10	2	0 55 – 1 37	16. Okt. – 30. Nov.
3	10	9	1	1 49 – 2 26	1. Nov. – 15. Dez. Dec
4	11	10	1	2 34 – 3 11	16. Nov. – 31. Dez.
5	14	12	2	3 19 – 4 01	1. Dez. – 15. Jan.
6	13	10	3	4 16 – 4 57	16. Dez. – 31. Jan.
7	12	12	–	5 06 – 5 57	1. Jan. – 15. Febr.
8	10	10	–	6 14 – 6 58	16. Jan. – 28. Febr.
9	9	9	–	7 13 – 7 47	1. Febr. – 15. März March
10	10	10	–	8 09 – 9 19	16. Febr. – 31. März
11	10	10	–	9 32 – 10 43	1. März – 15. Apr.
12	11	10	1	10 53 – 12 18	16. März – 30. Apr.
13	11	11	–	12 47 – 14 09	1. Apr. – 15. Mai May
14	11	10	1	14 20 – 15 22	16. Apr. – 31. Mai
15	10	8	2	15 42 – 16 36	1. Mai – 15. Juni June
16	8	8	–	17 01 – 17 17	16. Mai – 30. Juni
17	9	9	–	17 30 – 18 19	1. Juni – 15. Juli July
18	10	10	–	18 31 – 19 09	16. Juni – 31. Juli
19	9	9	–	19 18 – 19 43	1. Juli – 15. Aug.
20	12	10	2	19 55 – 20 46	16. Juli – 31. Aug.
21	12	12	–	20 59 – 21 31	1. Aug. – 15. Sept.
22	10	10	–	21 42 – 22 13	16. Aug. – 30. Sept.
23	11	10	1	22 25 – 22 54	1. Sept. – 15. Okt. Oct
24	10	10	–	23 04 – 23 48	16. Sept. – 31. Okt.
Sum	257	239	18		

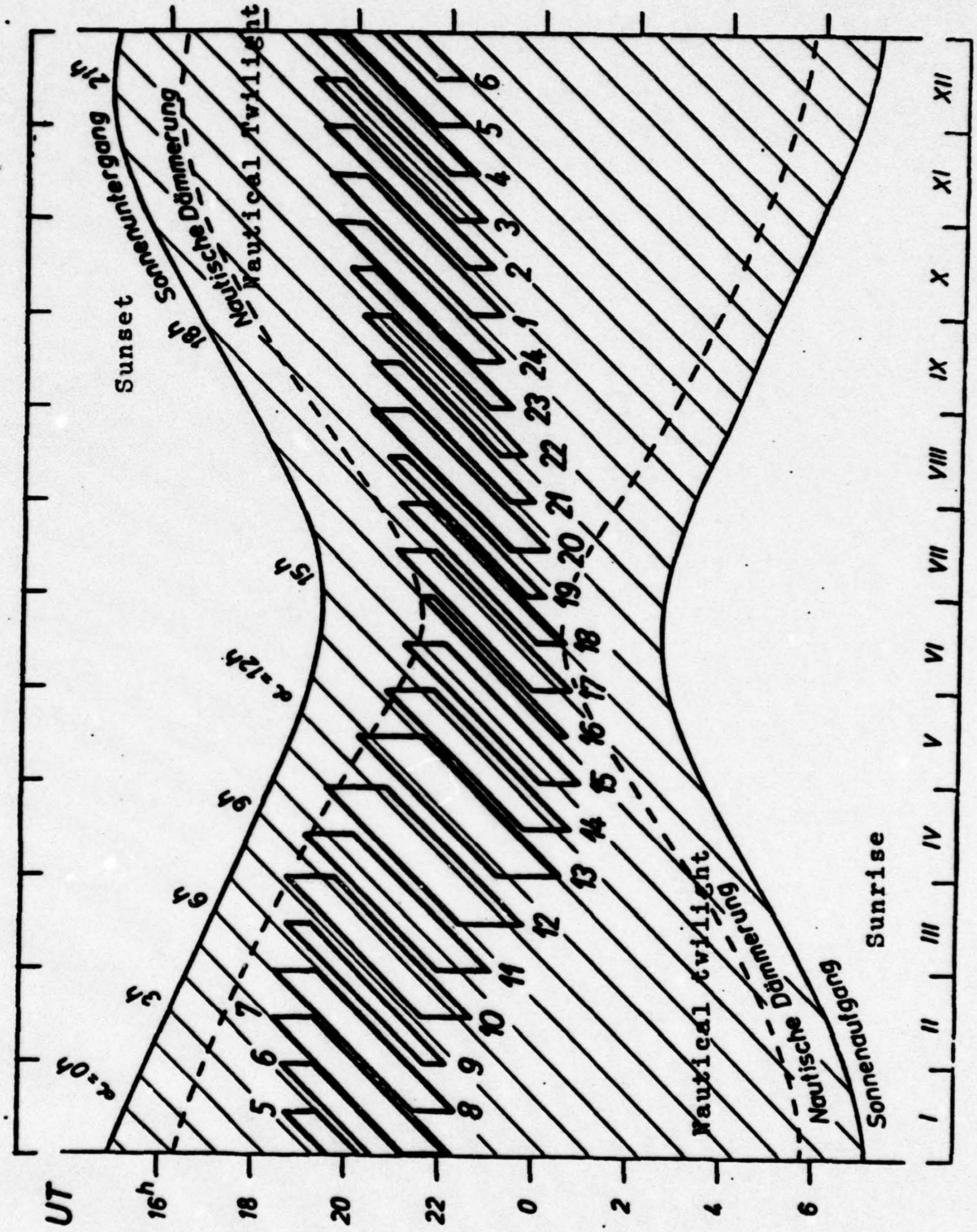

Figure 9. Program for the Observation of Groups 1 to 24

6. RESULTS OF THE TIME AND LATITUDE DETERMINATIONS

In the evaluation of the PZT observations, the rectangular coordinates of the star images on the photographic plate must first be determined. For this purpose, a ccordinate measuring apparatus with automatic data recording of VEB Carl Zeiss Jena is used. Prior to the measurement, the plate is approximately oriented in the measuring apparatus; the remaining orientation error is determined from the measured values by calculation. Additional starting data for the calculation of the time correction and of the latitude are the time position of the observation cycle in the time system UTC (ZIPE), which is measured during the observation, the apparent loci of the observed stars, as well as the star time for zero hours earth time. For the geogrphical longitude, the value

$$\lambda = 52^m 25\overset{s}{,}200 \text{ E}$$

is assumed. The arithmetic evaluation is carried out with the aid of the Robotron R 300 computer. The programming is based on the formulas summarized in Section 3.5.

For the evaluation of the observations of 1972 and 1973, the star loci of the AGK 3 (7) were initially used. The results of these observations served for the calculation of corrections for the AGK loci, which was already mentioned in the previous chapter. The revised catalog of the PZT stars (4) is the basis for the reduction of the observations since 1974. In addition, the observations of 1972 and 1973 were again reduced with the use of this catalog. The results for the years 1972 to 1974 are summarized in the appendix. Tables 2 and 3 give overviews of the groups and group combinations observed in the individual years. After consideration of the pole motion, using the pole coordination published by the Bureau International de l'Heure (BIH), an annual period shows clearly in the pattern of the latitude results of the years 1972 to 1974. An analysis in accordance with the equation

$$(62) \quad \varphi = \varphi_0 + s,$$

(t = fraction of year) led to the following results:

	a	b	c	d
1972	$-0\overset{s}{.}185$	$0\overset{s}{.}068$	$0\overset{s}{.}021$	$0\overset{s}{.}017$
	± 17	± 19	± 22	± 15
1973	-0,171	0,020	-0,048	-0,016
	± 17	± 18	± 17	± 18
1974	-0,236	-0,017	0,009	0,028
	± 14	± 16	± 15	± 15

Possible causes for the local z term could be, for example, residual declination errors of the form $\Delta\delta_{\alpha}$ or meteorological influences. Following the consideration of the pole motion and of the rotational variations, the results of the time determination shows no annual priods as obvious as the latitude determinations.

The quantities published in the BIH were used for the correction due to the pole motion and the rotational variations. Improvements for the assumed geographical latitude can be derived from the corrected time determinations. In this manner, the following mean values of the latitude of the PZT location are obtained for the individual years:

Longitude of the PZT station

1972	$52^{m}25\overset{s}{.}2307 \pm 0\overset{s}{.}0013$
1973	25,2303 ± 0,0015
1974	25,2534 ± 0,0019

The difference between the longitude values of 1972/1973 on the one hand and 1974 on the other hand is obviously caused by a change in the recording system at the beginning of 1974.

If the mean latitudes for the individual years is calculated from the corrected time determinations, the following values

Figure 2. Number of Observed Groups

Group	1972	1973	1974
1	7	6	0
2	5	4	1
3	5	4	2
4	4	4	4
5	4	3	2
6	1	6	3
7	1	5	1
8	1	5	1
9	2	8	2
10	3	8	4
11	3	7	6
12	6	7	6
13	4	6	6
14	6	5	6
15	3	9	6
16	3	9	5
17	4	8	3
18	5	11	2
19	2	11	4
20	2	9	9
21	1	11	9
22	4	10	9
23	5	6	6
24	7	5	5
Sum	88	167	102

are obtained, once with and once without consideration of the z term:

Latitude of the PZT station

	z	z
1972	52°24'24".861 ± 0".020	52°24'24".853 ± 0".013
1973	24,882 ± 0,015	24,891 ± 0,013
1974	24,925 ± 0,021	24,915 ± 0,011

The conventional coordinates of the PZT station, obtained from earlier observations, were used for a comparison with the PZT results (5):

Figure 3. Number of Observed Group Combinations

Combination	1972	1973	1974
1 - 2	3	3	0
2 - 3	4	3	1
3 - 4	3	0	2
4 - 5	4	2	2
5 - 6	1	3	1
6 - 7	0	3	1
7 - 8	1	3	1
8 - 9	0	4	0
9 - 10	1	5	2
10 - 11	3	5	2
11 - 12	2	5	5
12 - 13	2	3	2
13 - 14	4	1	2
14 - 15	3	5	4
15 - 16	0	7	3
16 - 17	3	3	2
17 - 18	3	6	1
18 - 19	2	7	1
19 - 20	1	6	4
20 - 21	0	5	8
21 - 22	0	6	5
22 - 23	4	4	4
23 - 24	4	2	5
24 - 1	6	3	0
Sur	54	94	58

$\lambda = 52^{m}25^{s}.239$ E, $\varphi = 52^{\circ}24'24''.36$ N.

The longitudinal values obtained from PZT observations evidence a satisfactory agreement with the conventional value, while there is a significant difference in the latitude. To clarify this discrepancy, the latitude was independently determined in accordance with the Sterneck method, using a Universal Instrument Wild T4. From this measurement, the latitude resulted as

$$\varphi = 52^{\circ}24'25''.03 \pm 0''.08.$$

This value can be considered a confirmation of the PZT result, while the conventional latitude, which was used for comparison purposes, is obviously defective.

7. ACCURACY INVESTIGATION

7.1. Errors of the Plate Dimensioning

The measuring error on the "Ascorecord", which is composed of the error of the alignment of the star with the measuring mark and the reading error, was calculated from differences of double measurements. The analysis of an extensive data store from the years 1972 and 1973 resulted in the total average for the mean error of an individual measurement ± 0.0032 mm. Apart from stars, which are brighter than $6^{m}.0$, there is no clear brightness dependence of the measuring error. In the case of stars, which are brighter than $6^{m}.0$, the measuring uncertainty is clearly greater (±0.0046 mm). If these bright stars are excluded from the considerations, the average error of an individual measurement amounts to ± 0.0028 mm and has equal magnitude for both coordinates.

A better quality of the photographic image was obtained from May 1974 on, by the use of the ZU2 plates and the improved focussing which was connected therewith. In this manner, the measuring error was reduced by about 30 percent and, for the one-time measurement of a coordinate, amounts to ± 0.0020 mm. In the evaluation of the PZT observations, the mean values of double measurements are introduced for the rectangular coordinates of the star images on the photographic plate. In accordance with these investigations, the measuring uncertainty of these quantities for both coordinates results as

$$m_x = m_y = \pm 0{,}0015 \text{ mm.}$$

7.2. Positional Errors of the Images on the Photographic Plate

The errors in the positions of the images on the photographic plate were determined by two different ways: on the one hand from the x differences of two images recorded in the same

position of the rotating head and, on the other hand, from the differences of the centroid coordinates, respectively the coordinate sums of the four images of a star. For the x differences, only the error component in the x direction can be determined. Starting with equation (29a), under consideration of the fact that

$$t_4 - t_2 = t_3 - t_1 \quad \text{and} \quad t_{M_4} - t_{M_2} = t_{M_3} - t_{M_1}$$

the relationship

$$(64) \quad (x_1 - x_3) \cos\theta + (y_1 - y_3) \sin\theta = (x_4 - x_2) \cos\theta + (y_4 - y_2)$$

respectively

$$(65) \quad x_1 + x_2 - x_3 - x_4 = (-y_1 - y_2 + y_3 + y_4) \tan\theta \, .$$

is obtained.

For the estimate of the amount of the expression $(-y_1 - y_2 + y_3 + y_4)$, we set the values of ω and θ equal to zero in equations (29b), and we obtain, through the formation of sums and differences

$$-y_1 - y_2 + y_3 + y_4 = b_y \left\{ (t_1 - t_m)^2 - (t_2 - t_m)^2 - (t_3 - t_m)^2 + (t_4 - t_m)^2 \right\} .$$

Through the insertion of the numerical values in (25), the result is for b_y

$$b_y = 0{,}48 \cdot 10^{-5} .$$

With the assumption that the star transit was observed symmetrically,

$$(t_1 - t_m)^2 = (t_4 - t_m)^2 = 2025$$

and

$$(t_2 - t_m)^2 = (t_3 - t_m)^2 = 225,$$

applies and thus

$$-y_1 - y_2 + y_3 + y_4 = 0{,}017 \text{ mm}.$$

In the evaluation, the PZT plates are generally so oriented

in the coordinate measuring apparatus that tan θ is less than 2×10^{-3}, so that the term $(-y_1 - y_2 + y_3 + y_4)$ tan θ can be neglected in formula (65). As a result, the condition

$$(66) \quad x_1 + x_2 - x_3 - x_4 = 0.$$

is obtained from (65).

As a result of errors in the x coordinates, this condition will not always be fulfilled by the measured values and, as an average, the mean error of an x coordinate can be determined, from the deviations Δ, for n stars, according to the following formula:

$$(67) \quad m'_x = \frac{1}{2}\sqrt{\frac{\Sigma \Delta^2}{n}}$$

The evaluation of about 250 stars resulted in

$$m'_x = \pm 0{,}0056 \text{ mm}.$$

If the measuring error, which is still contained in this value, is eliminated, the positional error in the x direction amounts to

$$m'_{Lx} = \pm 0{,}0054 \text{ mm}.$$

In the second method of the calculation of the positional errors, the coordinate sums of the four images of one star were used. In this case, the quantity θ can be neglected in equations (29a) and (29b), because it is generally sufficiently small prior to the measurement on the basis of the mentioned orientation of the plate. We then obtain the following relationships:

$$(68) \quad \begin{cases} x_0 - x_1 = a_x (t_1 - t_m) + b_x z_m (t_{H_1} - t_m), \\ x_0 - x_2 = -a_x (t_2 - t_m) - b_x z_m (t_{H_2} - t_m), \\ x_0 - x_3 = a_x (t_3 - t_m) + b_x z_m (t_{H_3} - t_m), \\ x_0 - x_4 = -a_x (t_4 - t_m) - b_x z_m (t_{H_4} - t_m) \end{cases}$$

and

$$
(69)\quad \begin{cases}
y_0 + y_1 = a_y\, z_m - b_y \left\{(t_1 - t_m)^2 + (t_{M_1} - t_m)\tau\right\}, \\
y_0 + y_2 = -a_y\, z_m + b_y \left\{(t_2 - t_m)^2 + (t_{M_1} - t_m)\tau\right\}, \\
y_0 + y_3 = a_y\, z_m - b_y \left\{(t_3 - t_m)^2 + (t_{M_1} - t_m)\tau\right\}, \\
y_0 + y_4 = -a_y\, z_m + b_y \left\{(t_4 - t_m)^2 + (t_{M_1} - t_m)\tau\right\}.
\end{cases}
$$

Through summing and transformation, the result is

$$(70)\quad x_1 + x_2 + x_3 + x_4 = 4x_0 + 2\,(a_x + b_x\, z_m)\,T$$

and

$$(71)\quad y_1 + y_2 + y_3 + y_4 = -4y_0 + b_y\,T\left\{2\tau + (t_1 - t_m) + (t_2 - t_m) + (t_3 - t_m) + \right.$$
$$\left. + (t_4 - t_m)\right\}.$$

For (70), we can write

$$(72)\quad x_1 + x_2 + x_3 + x_4 = K_x + 2b_x\, z_m\, T,$$

whereby $K_x = 4x_0 + 2a_x T$ is a constant value for all stars of a group. From (69), with sufficient approximation,

$$z_m = \frac{y_1 - y_2}{2a_y}$$

is obtained, and thus from (72)

$$(73)\quad K_x = x_1 + x_2 + x_3 + x_4 - \frac{b_x\,T}{a_y}\,(y_1 - y_2)$$

respectively, after the insertion of the numerical values

$$(74)\quad K_x = x_1 + x_2 + x_3 + x_4 - 0{,}1736\cdot 10^{-2}\,(y_1 - y_2).$$

Under consideration of equations (68),

$$(t_1 - t_m) + (t_2 - t_m) + (t_3 - t_m) + (t_4 - t_m) = \frac{1}{a_x}\,(x_2 - x_1 + x_4 - x_3)$$

can be written in (71) with adequate approximation. If,

furthermore, $-4y_0 = K_y$, it follows from (71)

$$(75)\quad y_1 + y_2 + y_3 + y_4 = K_y + \frac{b_y}{a_x} \cdot (x_2 - x_1 + x_4 - x_3).$$

Because the recordings are generally symmetrical to the meridian, the expression in parenthesis in (75) becomes very small, so that the second term on the right side of formula (75) can be neglected. Thus

$$(76)\quad K_y = y_1 + y_2 + y_3 + y_4.$$

The possibility of calculating mean coordinate errors results from equations (74) and (76). For this purpose, the average values must be formed from the values K_x and K_y for all n stars of a group:

$$(77)\quad \bar{K}_x = \frac{1}{n}\sum_{i=1}^{n} K_{x_i}, \qquad \bar{K}_y = \frac{1}{n}\sum_{i=1}^{n} K_{y_i}.$$

With the deviations of the individual values from the mean

$$v_{x_i} = \bar{K}_x - K_{x_i} \quad \text{and} \quad v_{y_i} = \bar{K}_y - K_{y_i}$$

the mean coordinate error for one image is obtained as

$$(78)\quad \bar{m}_x = \frac{1}{2}\sqrt{\frac{\sum v_x^2}{n-1}} \quad \text{and} \quad \bar{m}_y = \frac{1}{2}\sqrt{\frac{\sum v_y^2}{n-1}}.$$

As an average, the following errors resulted from the evalution of 50 plates, each with at least 10 stars:

$$\bar{m}_x = \pm 0{,}0063 \text{ mm}, \qquad \bar{m}_y = \pm 0{,}0064 \text{ mm}.$$

If the measuring error is again eliminated,

$$\bar{m}_{L_x} = \pm 0{,}0061 \text{ mm} \quad \text{respectively} \quad \bar{m}_{L_y} = \pm 0{,}0062 \text{ mm}.$$

remains as the positional error.

It is shown that both coordinates are obtained with equal accuracy. On the basis of the slight influence of the measuring error, a further improvement of the measuring accuracy is not

necessary. The principal error sources can obviously be found in refraction anomalies, scintillation, distortions of the photographic emulsion and instrumental error influences.

HØG (2) gives the following formula for the influence of the image motion (directional scintillation):

$$(79) \quad \sigma = 0\overset{''}{.}33\,(\tau + 0{,}65)^{-0{,}25}$$

(with τ = integration time). In the PZT, the integration time for one image amounts to τ = 20 seconds and, in accordance with (79), the influence of the directional scintillation becomes

$$\sigma = \pm 0\overset{''}{.}155$$

or, in the linear measure on the plate ± 0.003 mm.

7.3. Errors in Time Recording

The random error of time recording was calculated from differences of the of the time impulses of the PZT, with reference to the time scale UTC (ZIPE), for the first and third, respectively the second and fourth exposure. The accuracy of the recording an individual impulse amounts to ±0.2 ms. Four impulses are recorded for each star and, in the evaluation, the mean of the recorded impulses for all stars of a group is introduced. The random error of this mean value is less than 0.1 ms and plays a subordinate role in comparison with other error influences.

7.4. Errors of Time and Latitude Determinations

The influence of the positional errors on the final results, which was determined in Section 7.2, has already been investigated in Section 4.2. The mean errors obtained in the theoretical error considerations will now be compared with the errors resulting from time and latitude determinations. The mean errors for the observation of a star were calculated from

the deviations of the individual values from the group mean. The following average values resulted for the various years:

	$m_{\Delta u_o}$	m_{φ_o}
1972	$0^{s},0183$	$0'',167$
1973	0,0173	0,166
1974	0,0201	0,177

These results are in good agreement with the theoretically expected values, if it is taken into consideration that, in addition to the positional error, the final results are also influenced by the star corrdinate errors mentioned in Chapter 5. From the given values for the accuracy of the observation, the internal accuracy for a group of ten stars, which can be expected on the average, can be estimated at

$$m_{\Delta u_i} = \pm 0^{s},0059 \quad \text{and} \quad m_{\varphi_i} = \pm 0'',054.$$

The external accuracy was calculated from the deviations of the group means from the annual mean, whereby a reduction was first carried out because of the pole motion and the differences between the astronomically determined time and the coordinate earth time with the quantities published by the BIH. The external mean errors for the observation of a group have the following magnitudes:

	$m'_{\Delta u}$	m'_{φ}
1972	$0^{s},0125$	$0'',189$
1973	0,0185	0,196
1974	0,0184	0,209

Considering the local seasonal variations of the results, as taken into account for the latitude determinations according to formula (63) and for the time determinations in an analogous manner, these errors are reduced to the following values:

	$m_{\Delta u}$	m_{φ}
1972	$0^{s},0108$	$0'',110$
1973	0,0161	0,156
[illegible]	[illegible]	[illegible]

The average values of these errors for the years 1972 to 1974, in comparison with other PZT stations, are illustrated in Figure 10. The outer mean errors of the other stations were determined from the residual errors in the system of the BIH (6) for the year 1973. The errors of the time determination were reduced to the equator for all stations and transformed into seconds of arc. The cross in Figure 10 designates the average value of alloobservatories. It is shown that the quality of the Potsdam observations is equal to that of the other PZT stations when the local annual variations are taken into consideration, as this was done in the same manner in the BIH for the other stations.

All of the estimated values of the mean errors were determined with such a large number of degrees of freedom, that they can be considered expected values. Information about confidence intervals are therefore not necessary.

BIBLIOGRAPHY

1. Engelbrecht, J.: The Photographic Zenith Telescope (PZT) of the Babelsberg Observatory (Construction and Function), FEINGERAETETECHNIK, 15(1):8-12(1966).

2. Høg, E.: The Photoelectric Meridian Circle of Bergedorf/ Perth, ASTRON. UND ASTROPHYS., 19:27-40(1972).

3. Hohl, R. and Schomann, B.: Geodetic-Astronomical Location Determination for the Location of the Photographic Zenith Telescope in Babelsberg; Dissertation Techn. Univ. Dresden, 1973, unpublished.

4. Meinig, M.: Star Catalog for the Potsdam PZT, VEROEFF. ZENTRALINST. PHYSIK D. ERDE, Potsdam 37 (1976).

5. Struve, H.: The New Berlin Observatory in Babelsberg, VEROEFF. STERNWARTE BERLIN-BABELSBERG, Vol III, No. 1, Berlin 1919.

6. Bureau International de l'Heure; Rotation of the Earth, Processed Observations and Remainders in 1973.

7. ... Third Catalog of the Astronomical Society, Zone +52°, Computer Print-Out of the Star Data Center Strassbourg (1972).

OTHER LITERATURE

Pauscher, H.: Theory and Reduction Method for the Babelsberg PZT (unpublished manuscript).

Schuler, W.: Theoretical and Experimental Study of the Photographic Zenith Telescope (PZT) of Neuchatel; Geneva: EDITION MEDICINE & HYGIENE, 1967.

Takagi, S.: Geometry of the Setting Errors of the PZT, PUBL. INTERNAT. LATITUDE OBSERV. MIZUSAWA 3:137-149(1961).

Thomas, D. V.: Photographic Zenith Tube, Instrument and Method of Reduction, ROY. OBSERV. BULL. No. 81(1964).

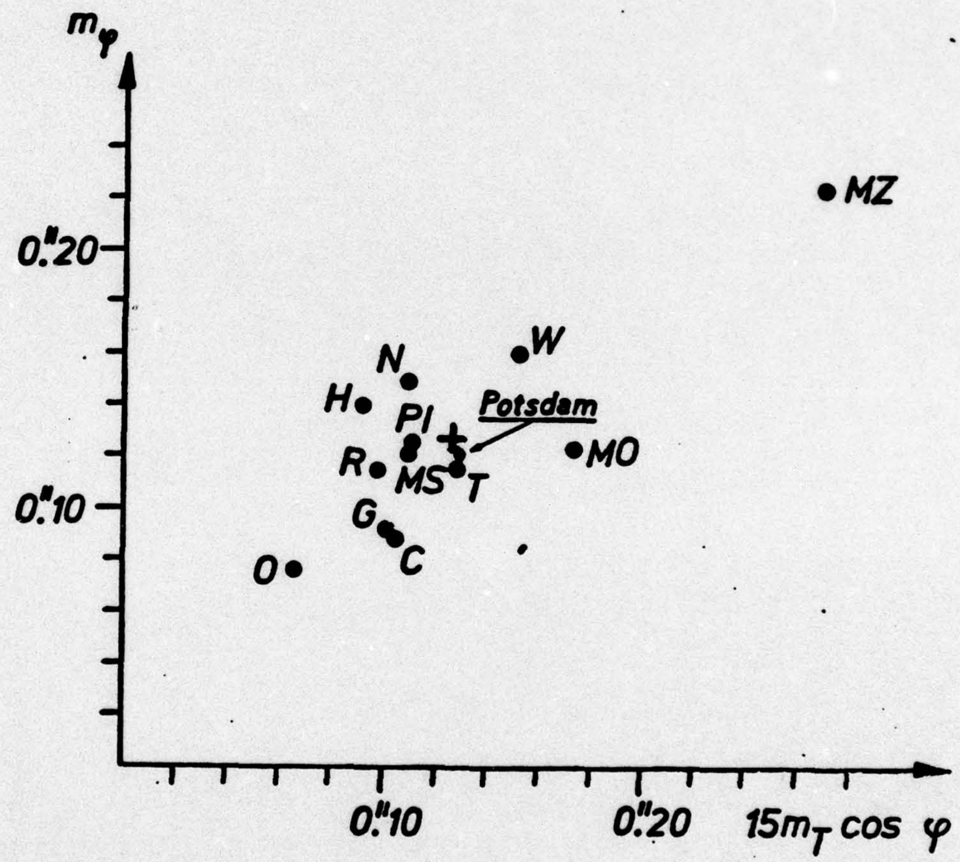

Figure 10. Comparison of Accuracy with Other PZT Stations

ATTACHMENT: Results of Experiments

Column 1 Sequential Number

2 Date: Month, Day

3 Modified Julian Date for the Mean of the Observation

4 Group Number

5 Number of Stars of the Time Determination

6 UTO(PZT) - UTC(ZIPE) [0.0001 second]

7 Mean Error of the Time Determination [0.001 second]

8 Number of Stars of the Latitude Determination

9 Observed Latitude

10 Mean Error of the Latitude [0.001 second]

Nr.	D	MJD	Gr	n	ΔU	$m_{\Delta U}$	n	φ	m_{φ}
1	2	3	4	5	6	7	8	9	10
	1972							52°24'	
1	02 02	41 349.83	7	7	-1094	59	7	24".677	28
2	02 02	349.87	8	6	-1206	61	6	24.631	70
3	03 13	389.80	9	9	-2441	58	9	24.623	53
4	03 13	389.86	10	8	-2500	45	8	24.592	53
5	03 13	389.90	11	7	-2492	102	7	24.547	67
6	03 14	390.86	10	6	-2168	52	6	24.496	83
7	03 14	390.90	11	4	-2434	74	4	24.466	84
8	03 14	390.95	12	6	-2555	73	6	24.524	64
9	03 24	400.83	10	7	-2910	93	7	24.500	32
10	03 24	400.88	11	8	-2816	69	8	24.509	47
11	03 24	400.93	12	9	-2656	44	9	24.445	37
12	04 24	431.84	12	11	-3801	77	11	24.357	43
13	04 24	431.96	13	6	-3840	71	6	24.306	66
14	04 25	432.00	14	9	-3890	33	9	24.237	51
15	04 25	432.84	12	10	-3859	51	10	24.365	38
16	04 28	435.83	12	6	-3962	22	6	24.350	70
17	04 30	437.82	12	9	-3713	44	9	24.222	40
18	04 30	437.92	13	8	-3756	66	8	24.216	51
19	04 30	437.98	14	9	-3826	51	9	24.438	47
20	05 05	442.91	13	11	-3786	40	11	24.283	42
21	05 05	442.97	14	10	-3862	21	10	24.382	24
22	05 06	443.02	15	10	-3987	33	10	24.638	56
23	05 07	444.90	13	11	-4225	30	11	24.558	19
24	05 07	444.96	14	11	-4238	29	11	24.496	37
25	05 08	445.01	15	10	-4170	30	10	24.665	45
26	05 08	445.96	14	8	-3989	66	8	24.425	72
27	05 09	446.01	15	8	-3965	52	8	24.400	25
28	05 25	462.92	14	8	-4581	45	8	24.248	52
29	06 20	488.93	16	7	-5663	69	7	24.527	50
30	06 20	488.96	17	5	-5635	79	5	24.560	57
31	06 25	493.92	16	6	-5597	50	6	24.682	73
32	06 25	493.95	17	6	-5495	142	6	24.726	49
33	06 25	493.99	18	6	-5450	95	6	24.674	48
34	06 26	494.92	16	7	-5583	75	7	24.510	67
35	06 26	494.95	17	8	-5651	97	6	24.485	122
36	06 26	494.98	18	6	-5802	39	6	24.861	75
37	07 13	511.90	17	8	+3892	44	8	24.744	39
38	07 13	511.94	18	10	3727	132	10	24.712	34
39	07 13	511.97	19	9	3881	96	9	24.602	36
40	07 18	516.92	18	9	3864	63	9	24.600	82
41	07 18	516.99	20	12	3809	109	12	24.955	54
42	07 20	518.91	18	7	3599	106	7	24.798	94
43	07 20	518.95	19	6	3739	39	6	24.826	41

Nr.	D		MJD	Gr	n	ΔU	$m_{\Delta U}$	n	φ	m_{φ}
1	2		3	4	5	6	7	8	9	10
	1972								52°24'	
44	07	20	41 518.98	20	11	+3643	67	11	24!880	64
45	08	07	536.97	21	8	3269	71	8	24.790	53
46	09	27	587.86	22	9	1776	79	9	25.224	91
47	09	27	587.89	23	10	1805	109	10	25.237	78
48	09	27	587.92	24	9	1744	77	9	25.215	71
49	10	04	594.84	22	9	1503	44	9	25.127	52
50	10	04	594.87	23	10	1560	48	10	25.071	31
51	10	04	594.90	24	10	1565	64	10	24.992	30
52	10	04	594.94	1	12	1540	78	12	25.016	31
53	10	05	595.84	22	9	1522	33	8	25.135	74
54	10	05	595.87	23	10	1623	64	10	25.161	36
55	10	05	595.90	24	10	1550	26	10	25.189	25
56	10	05	595.94	1	10	1517	72	10	25.050	56
57	10	08	598.83	22	9	1567	42	9	25.109	44
58	10	08	598.86	23	10	1540	54	10	25.063	28
59	10	08	598.89	24	9	1521	48	10	25.056	42
60	10	08	598.93	1	10	1448	90	10	25.124	52
61	10	13	603.88	24	10	1185	82	10	25.170	40
62	10	13	603.92	1	10	1032	83	10	25.112	48
63	10	16	606.84	23	7	1220	75	6	25.087	56
64	10	18	608.86	24	10	1127	69	10	25.018	93
65	10	18	608.90	1	12	1138	49	12	24.895	89
66	10	18	608.94	2	9	1152	73	9	25.140	134
67	11	01	622.83	24	9	0470	61	9	25.183	96
68	11	01	622.86	1	11	0563	47	11	25.091	46
69	11	01	622.90	2	7	0529	53	7	25.127	87
70	11	01	622.94	3	6	0584	55	6	25.169	174
71	11	14	635.83	1	12	0276	45	12	25.188	44
72	11	14	635.87	2	12	0295	27	12	25.166	88
73	11	14	635.90	3	9	0311	62	9	25.076	31
74	12	11	662.79	2	11	-0795	43	11	24.980	30
75	12	11	662.83	3	9	-0892	60	9	24.958	56
76	12	11	662.86	4	7	-0707	80	7	25.093	48
77	12	11	662.90	5	14	-0834	46	14	24.915	49
78	12	12	663.83	3	9	-0768	51	9	25.000	70
79	12	12	663.86	4	11	-0828	64	11	24.954	35
80	12	12	663.89	5	14	-0728	58	14	25.035	53
81	12	16	667.78	2	11	-0995	60	11	25.225	71
82	12	16	667.82	3	10	-1035	67	10	25.292	31
83	12	16	667.85	4	10	-1106	45	10	25.079	61
84	12	16	667.88	5	14	-0953	54	14	25.217	49
85	12	20	671.84	4	11	-1131	57	11	25.227	75
86	12	20	671.87	5	13	-1189	54	13	25.230	60
87	12	20	671.91	6	13	-1124	67	13	25.200	55

54

Nr.	D		MJD	Gr	n	ΔU	$m_{\Delta U}$	n	φ	m_{φ}
1	2		3	4	5	6	7	8	9	10
	1973								52°24'	
88	01	02	41 684.80	4	11	+8537	81	11	25!021	79
89	01	02	684.84	5	10	8444	52	10	25.073	83
90	01	02	684.87	6	8	8378	109	8	25.071	72
91	01	02	684.91	7	12	8274	165	12	25.025	82
92	01	13	695.81	5	11	8124	71	11	25.064	64
93	01	13	695.84	6	13	8312	52	13	25.048	58
94	01	13	695.88	7	12	8184	77	12	25.097	45
95	01	22	704.81	6	11	7815	58	11	24.768	43
96	01	24	706.81	6	7	7830	61	7	24.993	64
97	01	24	706.85	7	11	7667	48	11	24.895	35
98	01	24	706.89	8	5	7822	96	5	24.950	75
99	02	13	726.80	7	10	7108	39	10	24.890	32
100	02	13	726.84	8	9	6934	91	9	24.869	43
101	02	13	726.88	9	9	7116	44	9	24.837	52
102	02	14	727.79	7	11	7130	68	11	24.859	45
103	02	14	727.84	8	10	7101	65	10	24.751	33
104	02	14	727.87	9	9	7005	40	9	24.703	56
105	02	26	739.81	8	9	6726	42	9	24.661	43
106	02	26	739.84	9	9	6727	44	9	24.631	31
107	02	26	739.90	10	10	6708	34	10	24.588	64
108	02	27	740.80	8	10	6563	45	9	24.603	68
109	02	27	740.84	9	8	6561	43	8	24.653	64
110	02	27	740.89	10	10	6620	40	10	24.602	39
111	03	09	750.81	9	9	6342	27	9	24.603	28
112	03	09	750.87	10	7	6266	58	7	24.504	81
113	03	13	754.80	9	9	6148	82	9	24.751	38
114	03	13	754.86	10	8	6126	33	8	24.784	56
115	03	13	754.91	11	10	6061	30	10	24.716	27
116	03	14	755.80	9	9	6061	31	9	24.767	46
117	03	15	756.79	9	9	5998	28	9	24.731	38
118	03	15	756.85	10	6	6025	33	6	24.703	45
119	03	15	756.90	11	10	5948	25	10	24.725	35
120	03	23	764.83	10	10	5790	40	10	24.602	55
121	03	23	764.88	11	10	5734	80	10	24.692	26
122	03	23	764.93	12	11	5881	40	11	24.678	40
123	03	28	769.81	10	6	5506	79	6	24.677	36
124	03	28	769.87	11	10	5580	25	10	24.781	41
125	03	28	769.92	12	11	5659	37	11	24.738	39
126	03	29	770.81	10	10	5570	29	10	24.718	63
127	03	29	770.86	11	10	5485	30	10	24.704	35
128	03	29	770.92	12	10	5614	54	10	24.624	92
129	04	03	775.90	12	10	5377	25	10	24.376	39
130	04	03	775.99	13	4	5328	51	4	24.519	42

Nr.	D	MJD	Gr	n	ΔU	$m_{\Delta U}$	n	φ	$m_φ$
1	2	3	4	5	6	7	8	9	10
	1973							59°24'	
131	04 08	41 780.84	11	9	+5346	46	9	24.582	30
132	04 08	780.89	12	11	5297	48	11	24.528	37
133	04 13	785.82	11	10	5111	54	10	24.717	24
134	04 13	785.87	12	11	4966	81	11	24.608	61
135	04 13	785.97	13	11	5122	37	11	24.622	45
136	04 23	795.84	12	10	4840	17	10	24.512	57
137	04 23	795.94	13	11	4907	41	11	24.478	29
138	05 06	808.92	13	6	4456	63	7	24.760	53
139	05 07	809.02	15	10	4557	77	10	24.683	38
140	05 15	817.89	13	6	3931	59	6	24.518	114
141	05 16	818.88	13	11	4270	56	11	24.560	53
142	05 16	818.94	14	11	4220	44	11	24.684	41
143	05 16	818.99	15	8	4219	41	8	24.730	57
144	05 17	819.03	16	6	4014	108	6	24.785	52
145	05 17	819.94	14	11	4098	45	11	24.617	51
146	05 17	819.98	15	10	4167	60	10	24.751	42
147	05 18	820.03	16	8	3888	33	8	24.955	95
148	05 18	820.93	14	11	4248	30	11	24.722	62
149	05 18	820.98	15	10	4221	39	10	24.945	48
150	05 19	821.02	16	8	4122	40	8	24.782	84
151	05 23	825.92	14	11	4029	48	11	24.414	35
152	05 23	825.97	15	9	4128	53	9	24.694	44
153	05 24	826.01	16	5	3934	60	5	24.847	31
154	05 29	831.90	14	11	4211	34	11	24.642	27
155	05 29	831.95	15	10	4196	33	10	24.747	46
156	05 29	831.99	16	7	3888	42	7	24.801	35
157	06 05	838.93	15	9	3545	50	9	24.658	55
158	06 06	839.00	17	7	3232	91	7	24.628	58
159	06 14	847.91	15	10	3136	67	10	24.537	33
160	06 14	847.95	16	6	3194	41	6	24.774	93
161	06 16	849.90	15	10	3458	53	10	24.363	46
162	06 16	849.94	16	8	3359	31	8	24.609	94
163	06 16	849.98	17	9	3234	95	9	24.672	63
164	06 17	850.01	18	6	3151	90	6	24.690	86
165	06 18	851.93	16	3	2961	26	3	24.857	7
166	06 18	851.96	17	7	2989	54	7	24.790	97
167	06 19	852.01	18	7	3026	84	7	24.784	48
168	06 19	852.93	16	5	3080	163	5	24.610	98
169	06 19	852.97	17	9	3009	47	9	24.802	115
170	06 20	853.00	18	7	2983	83	7	24.701	39
171	06 20	854.00	18	6	2925	86	6	24.673	107
172	07 04	867.96	18	8	2559	79	8	24.751	56
173	07 04	867.95	19	6	2724	57	6	24.708	68

Nr.	D		MJD	Gr	n	ΔU	$m_{\Delta U}$	n	φ	m_φ
1	2		3	4	5	6	7	8	9	10
	1973								52°24'	
174	07	05	41 868.93	17	7	+2716	61	7	24:800	82
175	07	05	868.96	18	4	2810	110	4	24.772	124
176	07	05	868.99	19	7	2690	47	6	24.794	138
177	07	09	872.91	17	8	2463	69	8	24.599	47
178	07	09	872.95	18	5	2484	72	5	24.670	53
179	07	09	872.98	19	7	2454	77	7	24.569	103
180	07	10	873.91	17	7	2724	103	7	24.554	46
181	07	16	879.90	17	7	2359	61	7	24.504	95
182	07	16	879.93	18	8	2348	102	8	24.584	47
183	07	16	879.96	19	8	2334	46	8	24.609	43
184	07	29	892.89	18	6	2159	105	6	24.521	133
185	07	29	892.92	19	6	2052	133	6	24.240	186
186	07	29	892.96	20	9	2143	36	9	23.939	69
187	07	30	893.89	18	6	2156	80	6	24.363	30
188	07	30	893.92	19	7	2147	36	7	24.440	41
189	07	30	893.96	20	11	1981	74	11	24.560	49
190	07	31	894.88	18	6	2091	83	6	24.564	90
191	07	31	894.92	19	7	2009	51	7	24.765	60
192	07	31	894.95	20	11	1964	47	11	24.804	50
193	08	06	900.90	19	4	1962	142	6	24.942	79
194	08	06	900.94	20	9	1921	62	9	25.020	47
195	08	12	906.88	19	7	1759	45	7	25.060	106
196	08	12	906.92	20	11	1707	70	11	25.131	41
197	08	12	906.96	21	-	-	-	6	24.946	83
198	08	13	907.88	19	6	1541	112	6	25.013	99
199	08	13	907.95	21	5	1771	100	7	25.143	66
200	08	15	909.88	19	6	1583	77	6	25.135	47
201	08	15	909.91	20	10	1650	26	10	25.190	51
202	08	15	909.95	21	7	1709	88	7	25.139	72
203	08	15	909.98	22	4	1628	101	4	25.206	104
204	08	21	915.90	20	11	1447	31	11	25.028	59
205	08	21	915.93	21	9	1358	40	11	24.898	42
206	08	21	915.96	22	3	1438	96	8	24.936	55
207	08	22	916.89	20	11	0953	59	11	25.049	53
208	08	22	916.93	21	6	0857	79	6	24.940	41
209	08	23	917.89	20	11	0910	62	11	25.088	67
210	08	23	917.93	21	9	0874	35	9	25.065	57
211	08	23	917.96	22	5	1200	71	5	25.016	89
212	08	27	921.92	21	10	1116	57	10	24.874	83
213	08	27	921.94	22	-	-	-	6	24.730	112
214	09	04	929.90	21	6	1419	140	6	24.976	82
215	09	04	929.92	22	-	-	-	5	25.027	105
216	09	04	929.95	23	5	1362	38	5	24.912	52

Nr.	D		MJD	Gr	n	ΔU	$m_{\Delta U}$	n	φ	$m_φ$
1	2		3	4	5	6	7	8	9	10
	1973								52°24'	
217	09	10	41 935.87	21	4	+0868	69	5	24.800	40
218	09	14	939.86	21	10	0719	89	10	25.068	48
219	09	14	939.93	23	7	0953	68	7	24.981	56
220	09	15	940.86	21	10	0782	59	9	25.004	44
221	09	15	940.89	22	10	0850	57	10	24.863	44
222	09	15	940.92	23	9	0806	33	9	24.971	39
223	09	16	941.89	22	5	1068	33	5	24.924	65
224	09	16	941.92	23	8	0995	39	8	25.010	48
225	10	01	956.85	22	-	-	-	5	25.038	51
226	10	01	956.88	23	-	-	-	8	24.986	41
227	10	01	956.91	24	-	-	-	5	25.123	37
228	10	04	959.84	22	8	0541	53	8	25.033	65
229	10	04	959.90	24	7	0463	55	7	25.006	82
230	10	04	959.94	1	4	0349	90	5	25.189	71
231	10	06	961.84	22	7	0490	45	7	25.035	61
232	10	12	967.84	23	4	-0375	115	4	25.012	59
233	10	12	967.88	24	5	0004	105	5	24.953	105
234	10	12	967.92	1	8	0201	83	8	25.164	57
235	10	28	983.84	24	3	-0600	55	3	25.184	64
236	10	28	983.90	2	4	-0256	41	4	24.971	60
237	11	02	988.82	24	8	-0551	65	8	25.169	94
238	11	02	988.86	1	9	-0650	62	9	25.082	57
239	11	02	988.90	2	11	-0716	82	11	25.065	63
240	11	02	988.94	3	6	-0694	49	6	25.065	74
241	11	03	989.86	1	11	-0684	69	11	25.119	63
242	11	03	989.90	2	10	-0613	125	10	24.921	55
243	11	03	989.93	3	6	-0776	67	6	25.092	65
244	11	14	42 000.83	1	11	-1102	100	11	25.007	54
245	11	14	000.87	2	10	-0908	70	10	25.086	43
246	11	14	000.90	3	7	-0932	60	7	25.147	60
247	11	22	008.85	2	6	-1465	25	6	24.934	82
248	12	05	021.84	3	5	-1608	75	5	24.993	57
249	12	18	034.84	4	5	-1890	99	5	25.159	86
250	12	18	034.88	5	13	-1827	46	13	25.011	54
251	12	18	034.91	6	12	-1889	50	12	24.902	32
252	12	19	035.84	4	11	-2042	50	11	25.009	45
253	12	19	035.91	6	5	-1722	37	5	25.016	75
254	12	30	046.81	4	-	-	-	7	24.964	63

Nr.	D	MJD	Gr	n	ΔU	$m_{\Delta U}$	n	φ	m_{φ}
1	2	3	4	5	6	7	8	9	10
	1974							52°24'	
255	01 26	42 073.80	6	5	+6606	229	5	25.106	126
256	01 30	077.80	6	6	7131	77	6	24.883	115
257	01 30	077.84	7	-	-	-	5	24.805	71
258	01 30	077.88	8	5	6719	262	5	24.803	42
259	02 27	105.84	9	4	6196	91	4	24.875	92
260	02 27	105.89	10	7	5874	61	7	24.894	67
261	03 07	113.82	9	4	5822	68	4	24.657	77
262	03 07	113.86	10	4	5846	82	5	24.628	93
263	03 21	127.83	10	6	5371	57	6	24.634	78
264	03 21	127.89	11	9	5425	74	9	24.738	49
265	03 27	133.82	10	10	5235	75	10	24.562	72
266	03 27	133.87	11	9	5260	69	10	24.537	61
267	03 27	133.92	12	7	5285	97	7	24.559	103
268	04 01	138.86	11	9	5015	46	9	24.652	103
269	04 01	138.91	12	5	5282	101	5	24.537	76
270	04 03	140.85	11	8	5164	85	8	24.644	136
271	04 03	140.91	12	8	5242	44	8	24.639	59
272	04 04	141.01	13	8	5202	85	8	24.690	76
273	04 08	145.84	11	10	4796	48	10	24.665	49
274	04 08	145.89	12	11	4876	51	11	24.594	64
275	04 08	145.99	13	11	4852	70	11	24.567	55
276	04 09	146.84	11	10	4723	54	10	24.610	69
277	04 09	146.89	12	10	4982	47	11	24.543	59
278	04 26	163.84	12	7	4415	42	7	24.764	62
279	05 02	169.92	13	7	4219	79	7	24.554	57
280	05 02	169.96	14	3	4174	81	3	24.547	84
281	05 03	170.02	15	-	-	-	5	24.326	38
282	05 07	174.91	13	9	4105	72	9	24.453	42
283	05 07	174.96	14	8	3954	75	8	24.601	95
284	05 08	175.01	15	9	3782	37	9	24.819	76
285	05 10	177.90	13	10	4027	119	10	24.664	75
286	05 15	182.88	13	6	3945	48	10	24.783	57
287	05 15	182.99	15	8	3893	85	8	24.834	73
288	05 17	184.93	14	7	3789	63	7	24.603	36
289	05 24	191.92	14	11	3913	49	11	24.577	53
290	05 24	191.96	15	10	3924	37	10	24.791	59
291	05 30	197.90	14	8	3616	79	8	24.627	45
292	05 30	197.95	15	8	3659	45	8	24.798	27
293	05 30	197.99	16	8	3510	68	8	24.906	61
294	06 05	203.93	15	9	3564	29	9	24.808	50
295	06 05	203.97	16	8	3306	42	8	24.797	36
296	06 06	204.01	17	7	3277	34	7	24.803	31
297	06 15	213.90	15	6	3439	72	6	24.874	78

Nr.	D		MJD	Gr	n	ΔU	$m_{\Delta U}$	n	φ	m_φ
1	2		3	4	5	6	7	8	9	10
	1974								52°24'	
298	06	15	42 213.94	16	3	+2960	43	3	24."971	114
299	06	15	213.97	17	5	2844	79	5	24.871	114
300	06	17	215.94	16	5	3008	77	5	25.046	67
301	06	23	221.92	16	6	2690	38	6	24.655	43
302	07	02	230.93	17	9	2691	71	9	24.781	51
303	07	02	230.96	18	-	-	-	8	24.814	140
304	07	22	250.91	18	9	1946	41	9	24.897	77
305	07	22	250.94	19	8	1950	56	8	24.966	51
306	07	22	250.98	20	9	2070	94	9	25.149	56
307	08	07	266.90	19	9	1706	40	9	25.016	76
308	08	07	266.93	20	12	1740	79	12	25.035	52
309	08	07	266.97	21	11	1753	58	11	25.063	57
310	08	11	270.89	19	9	1659	43	9	24.946	58
311	08	11	270.92	20	10	1614	103	10	25.033	64
312	08	11	270.96	21	9	1376	56	9	25.168	39
313	08	15	274.88	19	9	1366	46	9	24.993	64
314	08	15	274.91	20	12	1432	93	12	25.179	61
315	08	15	274.95	21	11	1717	129	12	25.167	65
316	08	16	275.91	20	12	1524	116	12	25.108	42
317	08	16	275.95	21	12	1637	69	12	25.126	65
318	08	16	275.98	22	10	1435	40	10	25.001	54
319	08	23	282.89	20	12	1301	89	12	24.998	43
320	08	23	282.93	21	12	1128	55	12	25.030	22
321	08	23	282.96	22	10	1289	40	10	24.995	38
322	08	24	283.89	20	12	1335	80	12	25.098	49
323	08	24	283.92	21	12	1231	29	12	25.002	42
324	08	24	283.95	22	9	1418	50	9	24.966	39
325	08	29	288.87	20	12	1233	55	12	25.106	34
326	08	29	288.91	21	12	1168	39	12	24.998	60
327	08	29	288.94	22	10	1353	41	10	24.969	34
328	09	02	292.86	20	12	1172	79	12	25.094	46
329	09	02	292.90	21	11	1068	56	11	25.125	37
330	09	02	292.93	22	10	1294	39	10	25.045	26
331	09	02	292.95	23	6	1228	80	6	25.168	20
332	09	04	294.89	21	8	1089	44	8	25.220	26
333	09	20	310.88	22	10	0966	78	10	25.073	57
334	09	20	310.91	23	11	0880	55	11	25.157	37
335	09	20	310.94	24	8	0653	46	8	25.151	49
336	09	25	315.87	22	8	0964	98	8	25.144	100
337	09	29	319.85	22	6	0612	139	6	25.034	53
338	09	29	319.88	23	11	0740	62	11	25.352	45
339	09	29	319.91	24	10	0420	74	10	25.271	63
340	09	30	320.85	22	10	0539	44	10	25.016	51

60

Nr.	D	MJD	Gr	n	ΔU	$m_{ΔU}$	n	φ	$m_φ$
1	2	3	4	5	6	7	8	9	10
	1975							52°24'	
341	09 30	42 320.89	23	5	+0414	147	5	25"062	47
342	09 30	320.92	24	8	0358	23	8	25.090	72
343	10 02	322.88	23	11	0471	36	11	25.212	47
344	10 02	322.90	24	9	0383	36	9	25.108	33
345	10 11	331.85	23	9	0304	60	9	25.075	56
346	10 11	331.88	24	5	0250	89	5	25.057	119
347	11 20	371.86	2	6	-1442	98	6	24.929	109
348	11 20	371.89	3	9	-1411	53	9	24.881	79
349	11 20	371.92	4	10	-1195	157	10	24.843	127
350	12 03	384.85	3	10	-1542	64	10	24.871	73
351	12 03	384.88	4	11	-1432	46	11	24.872	65
352	12 03	384.92	5	13	-1429	66	13	24.814	50
353	12 22	403.83	4	10	-1911	66	10	24.800	60
354	12 23	404.83	4	11	-1911	61	11	24.883	46
355	12 23	404.86	5	14	-1999	63	14	24.910	36
356	12 23	404.90	6	8	-2037	51	8	24.923	55